

CHARACTERIZING BIOMASS BURNING IN SHRUB-STEPPE:
BURNED AREA AND SEASONAL TRACE GAS EMISSION FACTORS

A Thesis

Presented in Partial Fulfillment of the Requirements for the

Degree of Master of Science

with a

Major in Natural Resources

in the

College of Graduate Studies

University of Idaho

by

Aaron M. Sparks

May 2014

Major Professor: Alistair M. S. Smith, Ph.D.

AUTHORIZATION TO SUBMIT THESIS

This thesis of Aaron M. Sparks, submitted for the degree of Master of Science with a major in Natural Resources and titled “Characterizing Biomass Burning in Shrub-steppe: Burned Area and Seasonal Trace Gas Emission Factors,” has been reviewed in final form. Permission, as indicated by the signatures and dates given below, is now granted to submit final copies to the College of Graduate Studies for approval.

Major Professor _____ Date _____
Dr. Alistair M. S. Smith

Committee
Members _____ Date _____
Dr. John D. Marshall

_____ Date _____
Dr. Robert J. Yokelson

Department
Administrator _____ Date _____
Dr. Anthony S. Davis

College of Natural
Resources Dean _____ Date _____
Dr. Kurt S. Pregitzer

Final Approval and Acceptance by the College of Graduate Studies

_____ Date _____
Dr. Jie Chen

ABSTRACT

Fire is one of the most influential disturbance agents in the Earth's terrestrial and atmospheric environments; it alters availability of nutrients for plants and directly contributes to the concentration of trace gases and particulates in the atmosphere. Global climate change, coupled with increasing use of prescribed fire, provides an ongoing need for monitoring emission fluxes of trace gases to the atmosphere. As plant communities shift due to changing temperatures and fire frequency (e.g., the cheatgrass-sagebrush systems in the Great Basin, United States), increased knowledge of the variability in timing and quantity of fire emissions is necessary. The research within this thesis is focused on characterizing the uncertainty associated with the calculation of emission flux from shrub-steppe ecosystems. Specifically, this research 1) quantifies the uncertainty within the most widely applied burned area mapping product that is used in United States shrub-steppe ecosystems, 2) characterizes season variability in nitrogenous and carbonaceous trace gas emissions for shrub-steppe systems observed from laboratory burns, and finally 3) discusses possible underlying mechanisms for these observed results.

ACKNOWLEDGEMENTS

I would like to first express my gratitude to my major advisor, Alistair Smith, for his guidance and support. Coming into this program I had started to slip into a world of mediocrity and I thank Alistair for pushing me to become not only a scientist but a great scientist. Alistair has also helped renew my curiosity in the natural world by challenging and supporting my ideas and encouraging me to have a healthy balance of confidence and skepticism. I would like to thank him for renewing this interest and helping me reach my full potential.

I extend my gratitude to John Marshall and Robert Yokelson. This thesis would be a mere shadow of what it is today without your insightful ideas and suggestions. Thank you for being patient and lending some of your time to helping me achieve this goal.

I also thank my family and friends for being there for me. I may poorly convey what I do and study, but thanks for listening and offering support. I especially thank Amanda Argona, my best friend and love of my life. Thank you for being patient during the stressful times and for the countless hours you spent helping me with this project.

A debt of thanks is owed to the Columbia National Wildlife Refuge, especially Rich Albers and Gordon Warrick, for their help. This work would not have been possible without their interest and support of this research. Additionally, I thank Stephen Baker at the Missoula Fire Science Lab for his chemistry expertise and for lending us the trace gas analyzers necessary for this project. And most importantly, I thank the National Aeronautics and Space Administration (NASA) for partially funding this work under award NNX11AO24G.

TABLE OF CONTENTS

Authorization to Submit Thesis	ii
Abstract	iii
Acknowledgements	iv
Table of Contents	v
List of Tables	vii
List of Figures	viii
CHAPTER 1: An Overview of Burned Area and Trace Gas Emission Factors	1
Introduction	1
Study Area	6
Scope and Objectives	7
Chapter Summaries	7
References	9
Tables	17
Figures	19
CHAPTER 2: An Accuracy Assessment of the MTBS Burned Area Product for Shrub-steppe Fires in the Northern Great Basin, United States	22
Abstract	22
Introduction	22
Datasets	23
Methods	25
Results and Discussion	28
Conclusions	30
Acknowledgements	30
References	31
Tables	35
Figures	36

CHAPTER 3: Evaluating the Dependence of Sagebrush Trace Gas Emission Factors on Seasonal Phenology	39
Abstract	39
Introduction	39
Methods	42
Results and Discussion	45
Conclusions	47
Acknowledgements	48
References	49
Tables	52
Figures	54
Appendices	57
Appendix A: Emissions Data from Shrub-steppe Fires: Bluebunch Wheatgrass and Cheatgrass	57
Appendix B: Quantification of Fuel Moisture Effects on Biomass Consumed Derived from Fire Radiative Energy Retrievals	62

LIST OF TABLES

Chapter 1 Tables	17
Table 1. Common spectral indices used for burned area mapping	17
Table 2. Average emission factors of major carbonaceous and nitrogenous species and PM _{2.5} for savanna, tropical forest, boreal, and temperate biomes	18
Chapter 2 Tables	35
Table 1. Burned area accuracy assessment of the optimal CSI, MIRBI and RdNBR thresholds, MTBS perimeters, and CSI, MIRBI and RdNBR thresholds constrained by MTBS perimeters for the four fires. All accuracies are expressed as percent	35
Chapter 3 Tables	52
Table 1. Summary of big sagebrush moisture content, elemental analysis, and fuel consumption measurements	52
Table 2. Relationships between CO ₂ and CO emission factors (this study) and big sagebrush foliar constituents (Kelsey et al., 1982)	53

LIST OF FIGURES

Chapter 1 Figures	19
Figure 1. Seasonal dependence of a) MCE for African grassland and woodland fires, b) EF_{CO_2} from grassland fires, and c) EF_{CO} from grassland fires (adapted from Korontzi et al. 2003).....	19
Figure 2. Predicted North American biome distribution shifts from, a) present day to, b) year 2090 (Rehfeldt et al., 2012). Red outline is approximate boundary of Great Basin region. Great Basin region biomes: white = Great Basin shrub-grassland, dull purple = Rocky Mountain montane conifer forest, dark red = Great Basin conifer woodland, dark teal = Great Basin desert scrub, pink = Great Basin montane scrub, light teal = Mohave desert scrub, tan = Sonoran desert scrub.....	20
Figure 3. Progression of thesis research and future work avenues.....	21
Chapter 2 Figures	36
Figure 1. Map of western United States forested and rangeland extent, which include shrub steppe, and the location of the investigated fires (Burnt, Dry Creek Complex, Hogups, and Scorpio). The Burnt fire burned 3,499 ha in south-central Idaho in early July, the Dry Creek Complex burned 18,592 ha in south-central Washington, the Hogups fire burned 10,425 ha in northwest Utah in early August, and the Scorpio fire burned 5,789 ha in northwest Utah in late June	36
Figure 2. Remote sensing imagery for the (a) Burnt fire and (b) Dry Creek Complex fire showing a Landsat TM false color composite (R:band 7, G: band 4, B:band 5), the visually interpreted reference data, MTBS-perimeter with commission errors shown in red, and RdNBR, CSI, and MIRBI burned area maps displaying correctly classified burned area (white) and non-burned area (black), commission (red) and omission errors (green) inside the burn perimeter, and commission errors (yellow) outside the burn perimeter. Threshold values used for the classification are reported for each index	37
Figure 3. Remote sensing imagery for the (a) Hogups fire and (b) Scorpio fire showing a 7:4:5 band false color composite, the manually-derived burn area map, MTBS-perimeter with commission errors overlaid, and RdNBR, CSI, and MIRBI burned area maps displaying correctly classified burned area (white) and non-burned area (black), commission (red) and omission errors (green) inside the burn perimeter, and commission errors (yellow) outside the burn perimeter. Threshold levels are inset for each of the indexes	38

Chapter 3 Figures	54
Figure 1. Description of the study area including, a) extent of sagebrush in the Great Basin with fires from 1910-2011 and urban areas >3,000 people overlaid ...	54
Figure 2. Emissions data including, a) climate data of study site (from Columbia National Wildlife Refuge RAWS station) and moisture content of sagebrush samples collected from May 5, 2013 to October 22, b) carbon and nitrogen content of samples, along with C:N ratio, c) seasonal CO ₂ and CO emission factors, d) seasonal NO, NO ₂ , and NO _x emission factors, e) carbon balance, f) nitrogen balance	55
Figure 3. Relationships between EF _{CO2} (this study) and sagebrush foliar crude fat and crude terpenoids (Kelsey et al., 1982)	56
Appendix A Figures	58
Figure 1. Emissions data including, a) climate data of study site (from Columbia National Wildlife Refuge RAWS station) and moisture content of bluebunch wheatgrass samples collected from May 5, 2013 to October 22, b) carbon content of samples (red = lower plant, blue = upper plant), along with C:N ratio, c) seasonal CO ₂ and CO emission factors (samples burned dry), d) seasonal CO ₂ and CO emission factors (samples burned at field moisture content (FMC)), e) carbon balance (samples burned dry), f) carbon balance (samples burned at FMC)	58
Figure 2. Emissions data including, a) climate data of study site (from Columbia National Wildlife Refuge RAWS station) and moisture content of bluebunch wheatgrass samples collected from May 5, 2013 to October 22, b) nitrogen content of samples (red = lower plant, blue = upper plant), along with C:N ratio, c) seasonal NO _x emission factors (samples burned dry), d) seasonal NO _x emission factors (samples burned at field moisture content (FMC)), e) nitrogen balance (samples burned dry), f) nitrogen balance (samples burned at FMC)	59
Figure 3. Emissions data including, a) climate data of study site (from Columbia National Wildlife Refuge RAWS station) and moisture content of cheatgrass samples collected from May 5, 2013 to October 22, b) carbon content of samples (red = lower plant, blue = upper plant), along with C:N ratio, c) seasonal CO ₂ and CO emission factors (samples burned dry), d) seasonal CO ₂ and CO emission factors (samples burned at field moisture content (FMC)), e) carbon balance (samples burned dry), f) carbon balance (samples burned at FMC)	60
Figure 4. Emissions data including, a) climate data of study site (from Columbia National Wildlife Refuge RAWS station) and moisture content of cheatgrass samples collected from May 5, 2013 to October 22, b) nitrogen content of samples (red = lower plant, blue = upper plant), along with C:N ratio, c) seasonal NO _x emission factors (samples burned dry), d) seasonal NO _x emission factors (samples burned at field moisture content (FMC)), e) nitrogen balance (samples burned dry), f) nitrogen balance (samples burned at FMC)	61

Appendix B Figures 76

Figure 1. Relationship between fire radiant energy (FRE) biomass consumed (BC) for 15 dry (<0.01 W_C) pine needle experimental burns (closed circles). The best-fit linear regression passing through the origin ($BC=(0.325\pm0.008)*FRE$, $r^2=0.998$, $n=15$, $p<0.01$) is shown as a continuous line. The dashed line shows the BC predicted from the retrieved FRE using the conventional relationship described by [7] 76

Figure 2. The impact of water content, W_C , on the FRE per unit of biomass consumed (FRE/BC) for 24 experimental burns (closed circles). The regression of these data (solid line) is: $FRE/BC (MJ Kg^{-1}) = -5.32W_C + 3.025$ ($r^2=0.832$, $n=24$, $p<0.001$). The 95% confidence intervals for the gradient and intercept are ± 0.0105 and ± 0.079 respectively. The theoretical radiant heat budget per unit mass consumed [4] is shown as a dashed line 77

Figure 3. Impact of fuel water content W_C (dimensionless), on the relationship between retrieved FRE and biomass consumed (BC). Equation [8] is theoretically demonstrated for W_C values from 0-0.25 for the 15 dry pine fuel FRE retrievals illustrated in Fig. 1, and the resulting linear equations are plotted as diagonal lines. The % uncertainty is calculated for each W_C line by applying the 95% confidence intervals from the gradient and intercept coefficients in [8]. Only the error bars associated with 0.15 and 0.25 are shown for illustrative purposes. Pine needles do not burn if the water content is higher than ~ 0.26 . The reported equations values are derived from the current experimental data and are in close correspondence to the theoretical values that can be derived from [5] 78

Chapter 1

An Overview of Burned Area and Trace Gas Emission Factors

Introduction

Biomass burning is one of the dominant sources of emissions to the atmosphere (Andreae and Merlet, 2001; Yokelson et al., 2013). Quantifying the sources of uncertainty in these emissions is critical to further understanding the role of fires in biogeochemical processes, especially in the face of changing climate and plant communities. Fire emissions like carbon dioxide (CO₂), methane (CH₄), and black carbon (BC) have significant global warming effects, with CO₂ and BC each representing significant contributions to global warming (Jacobson, 2001b; Lashof and Ahuja, 1990). Other emissions like carbon monoxide (CO) and nitrogen oxide (NO_x) have been linked with tropospheric ozone (O₃) formation (Khalil and Rasmussen, 1988). CO and NO_x emissions from biomass burning represent ~26% and ~11%, respectively, of the total sources of these trace gases to the atmosphere (IPCC, 2013). The large contribution and influence of biomass burning emissions to atmospheric chemistry makes emission estimates crucial for determining air quality, especially in heavily populated areas where prescribed fire is prevalent (Chen et al., 2007; Reisen et al., 2011; Wiedinmyer et al., 2011).

The majority of studies seeking to quantify biomass burning emissions utilize an equation similar to (Sieler and Crutzen, 1980):

$$Emission\ flux_{(x)} = A \times B \times \frac{b}{100} \times EF_{(x)} \times C$$

where A = total area burned (ha), B = fuel load available to combust (kg m⁻²), b = fuel consumption (%), EF_x = emission factor (g kg⁻¹ fuel combusted), with EF_x usually expressed as a fire-averaged emission factor, and C converts units. Recently, a reduced formulation replaces B and b with the fuel combusted per unit area as defined by fire radiative energy studies (Freeborn et al., 2008; Smith et al., 2013; Wooster et al., 2005). Regardless of which formulation is applied, the uncertainty associated with each emission flux component needs to be understood. The following background section includes an overview of how burned area and emission factors are acquired and the uncertainty associated with these emission flux elements in the savanna and temperate biomes.

Background: Burned area and emission factor measurements

In the last few decades, burned area has typically been assessed using two methods: 1) manually, using a GPS (global positioning system) or topographic map on foot or aerial platform, and 2) via remote sensing imagery from aerial and satellite platform. The first technique has been observed to overestimate area burned of individual burns measured by ~18%, as unburned islands and fingers can be ignored in the mapping process (Amiro et al., 2001; French et al., 2004; Kolden and Weisburg, 2007). Despite this weakness, manually mapped area burned data can be the only burned area data available for fires pre-satellite data (~1984). The second technique, the use of remotely sensed imagery, provides an effective method for mapping area burned as the differences in reflective and thermal characteristics pre- and post-fire promote the use of spectral indices; dimensionless, radiometric measures that enhance sensitivity of a target object (charcoal) and normalize external and internal effects like sun angle, topography, etc (Running et al., 1994).

Surface reflective characteristics post-fire typically include a reduction in the visible (0.4-0.7 μm) to near-infrared (NIR: 0.8-1.2 μm) reflectance and an increase in short-wave infrared reflectance (SWIR) (Smith et al., 2007). Many spectral indices have been developed to take advantage of this difference to enhance the sensitivity of burned versus non-burned area (Table 1). NDVI (normalized difference vegetation index), NBR (normalized burn ratio), MIRBI (mid-infrared bi-spectral index), CSI (char soil index), BAI (burned area index), are some of the most commonly used spectral indices for burned area mapping (Chuvieco et al., 2001; Kasischke and French, 1995; Lopez-Garcia and Caselles, 1991; Rouse et al., 1974; Smith et al., 2005; Trigg and Flasse, 2001). Additional indices are covered in detail in several reviews on burned area mapping methods (Periera, 2003; Lentile et al., 2006). Semi-automated methods that use spectral indices have also been developed to map burned area, including MTBS (monitoring trends in burn severity) (Eidenshink et al., 2007).

Emission factors are another key component of the emission flux calculation. While there are several different ways to report emissions, emission factors provide one of the more useful metrics for reporting emissions of trace gases and particulate matter from biomass burning. Emission factors are defined as the following (Ward, 1979):

$$EF_{(x)} = \frac{M_{(x)}}{M_{(biomass)}}$$

where $M_{(x)}$ is the total mass (g) of species $_{(x)}$ emitted and $M_{(biomass)}$ is the mass (kg) of the consumed biomass for time period 't'. Calculation of emission factors usually follows the carbon mass balance method, detailed in Ward (1979) and Yokelson et al. (1999). The carbon mass balance method provides a good estimate of emissions, however, it assumes that all combusted carbon is volatilized and measured, carbon content of the fuel is known, and the smoke is adequately mixed.

Emission factors can be separated into flaming and smoldering combustion emission factors or presented as fire-average emission factors. It is difficult to separate flaming and smoldering combustion emission factors as both processes occur simultaneously in a given area. However, combined with combustion efficiency or modified combustion efficiency (MCE), detailed in Ward and Radke (1993), we can approximate these two combustion processes as flaming combustion products are generally positively correlated with MCE and smoldering combustion products are generally negatively correlated. In certain cases, however, several studies have found that fuel composition (i.e. nitrogen and sulfur content) can mask MCE (Burling et al., 2010; Yokelson et al., 2011).

There have been numerous field studies, including many large field campaigns (i.e. SAFARI, BASE-A, TROFFEE), partially focused on reducing uncertainties in biomass burning emission factors (Fearnside et al., 1993; Scholes et al., 1996; Yokelson et al., 2007). There have also been many laboratory biomass burning studies (Burling et al., 2010; Freeborn et al., 2008; Yokelson et al., 1999), which have proven to be equally helpful in increasing our emissions knowledge (Yokelson et al., 2013). Most of these studies have been focused on a brief period during the burn season (i.e. 1-2 months) with very few studies measuring emission factor variation over an entire burn season (Hoffa et al., 1999; Korontzi et al., 2003; Mebust et al., 2013).

Sources of global biomass burning emissions: Savanna ecosystems

One of the largest contributors to global biomass burning gas emissions is the savanna biome in the tropics, located between ~15°N and ~20°S. It is estimated that 44-60% of trace gas emissions in the tropics originate from the burning of savannas (van der Werf et al.,

2010). This region consists of grass-dominated savanna and woodland savanna, with the majority of the biome's extent located in southern Africa and South America. Fires in this system occur predominantly during the dry season, ~May through October (Trollope 1984; Scholes et al., 1996), with ~66% of total burning occurring in southern Africa (Hao et al., 1990). Fire frequency can vary from 1 to 8 years, with more frequent burning (burn annually or biannually) occurring in the higher fuel loads of humid savanna and less frequent (burn every 4 to 8 years) in the lower fuel loads of dry savanna (Trollope, 1984).

Area burned within the savanna biome can vary considerably from study to study and year to year. Area burned estimates range from ~116-168 Mha yr⁻¹ (Van der werf et al., 2003; Scholes et al., 1996) to ~650-750 Mha yr⁻¹ (Levine and Cofer, 2000). One reason for this high level of uncertainty is the lack of reliable ground data. Area burned and fire frequency records are hard to find except for national parks, which tend to have highly regulated fire management plans (Scholes et al., 1996). Recently, semi-automated burned area mapping methods using Moderate Resolution Imaging Spectroradiometer (MODIS) data have been successfully used to map large fires in this region (Roy et al., 2005, 2008).

Emission factors for the studies reviewed were typically derived from airborne, ground, or laboratory-based sampling. Regardless of sampling platform, most studies produced very similar CO₂ emission factors ($\bar{x} = 1706 \text{ g kg}^{-1}$) with relatively low uncertainty (coefficient of variation (CV) = $\pm 5\%$) (Table 2). Nitrogenous emission factors were far more uncertain, with CV ranging from $\pm 18\%$ to $\pm 53\%$. In general, airborne-based studies (Kaufman et al. 1992; Cofer et al. 1996; Ferek et al. 1998; Sinha et al. 2003; Yokelson et al. 2003; Sinha et al. 2004) estimated lower emission factors (with greater uncertainty) for smoldering combustion species, such as CO, CH₄, and NMHC, compared to ground based studies (Ward et al. 1992; Ward et al. 1996). In fact, average uncertainty was 1.5 to 2 times greater for airborne versus ground based sampling. This discrepancy between airborne and ground based samples could be due to the fact that most of the smoldering combustion emissions, which are dominantly produced at lower temperatures, remain closer to the ground (Urbanski et al. 2009). Conversely, flaming combustion emissions are lofted higher into the atmosphere through convective processes (Hurst et al. 1994a). Generally, in savannas the low emission factors of gases produced during smoldering combustion, such as CH₄, are

attributed to higher combustion efficiencies during burning (Yokelson, et al., 2003; Sinha et al., 2003; Akagi et al., 2011).

Most of the emission factor estimates in savanna ecosystems, regardless of location or sampling platform, have been concentrated in the late dry season months of August and September (Kaufman et al. 1992; Ward et al. 1992; Cofer et al. 1996; Bertschi et al. 2003; Yokelson et al. 2003; Keene et al. 2006). This time period encapsulates most of the burning, however, extensive burning also occurs in the early dry season for agricultural as well as fire prevention reasons. Generally, modified combustion efficiency increases through the burn season, from May to October. Korontzi et al. (2003) observed significant seasonal dependence for MCE and major carbonaceous species, especially in wooded savanna, where consumption of dried logs later in the season contributed to lower MCE and smoldering products (Figure 1). Higher moisture content of fuels in the early part of the burning season also contributes to the production of greater smoldering combustion emissions (Hoffa et al. 1999; Justice et al. 2002; Korontzi et al. 2003).

Sources of global biomass burning emissions: Temperate ecosystems

Temperate ecosystems have been thought to have a relatively low global contribution of biomass burning emissions. However, relatively few studies have looked at emissions from temperate ecosystems, with the United States being one of the few areas studied (Wiedinmyer and Hurteau, 2010). Temperate ecosystems studied include: temperate forests (Bertschi et al., 2003; Burling et al., 2011; Friedli et al., 2001; Urbanski et al., 2009; Yokelson et al., 1999), temperate grasslands (Urbanski et al., 2009; Yokelson et al., 2011), and chaparral (Burling et al., 2011; Friedli et al., 2001; Hegg et al., 1990; Laursen et al., 1992). Much of the biomass burning emissions in the United States and other temperate regions can be attributed to prescribed fire, which is closely controlled to protect air quality (Chen et al., 2007; Mutch, 1994; Neary, 2005; Reisen et al., 2011; Wiedinmyer and Hurteau, 2010). Similar to other major sources of biomass burning emissions, most of the studies looked at a small window (i.e. 1 to 2 months) throughout the year.

Burned area in temperate areas, especially in the United States, is fairly accurate due to increased interest in monitoring air quality and other fire influenced factors. The majority of studies in the United States use area burned estimates from either government agencies

(United States Forest Service, Bureau of Land Management, National Park Service) or use burned area mapping products produced by the Monitoring Trends in Burn Severity (MTBS) project. Recent studies have shown that MTBS data can be a large source of error when estimating emissions from temperate shrub-steppe ecosystems due to large burned area commission errors on and inside the fire perimeter (Sparks et al., in press). By including unburnt fingers and islands, these errors could significantly inflate the emission flux estimates produced for these ecosystem types.

Emission factors, and their associated uncertainty, in temperate ecosystems follow trends in other ecosystems. Generally, uncertainty associated with flaming combustion products such as CO₂ are relatively low (CV = ±2-16%) whereas smoldering combustion uncertainties are higher (CO, ±4-45%; CH₄, ±32-106%; NMHC, ±5-42%)(Table 2). Nitrogen oxides also have larger uncertainty associated with emission estimates (±12-52%). Similar to emission factor estimations from savanna ecosystems, airborne and lab measurements from temperate ecosystems differ from ground-based measurements. Generally, higher emission factors (\bar{x} = 180.5 g kg⁻¹ CO; 12.3 g kg⁻¹ CH₄) are reported for ground-based sampling than for airborne-based sampling (\bar{x} = 87 g kg⁻¹ CO; \bar{x} = 3.8 g kg⁻¹ CH₄) (Bertschi et al. 2003; Burling et al. 2010, 2011; Freeborn et al. 2008; Friedli et al. 2001; Hegg et al. 1990; Laursen et al. 1992; Urbanski et al. 2009; Yokelson et al. 1996, 1999, 2011).

Study Area

Shrub-steppe ecosystems, like those in the northern Great Basin, U.S., provide a good opportunity to study emission flux components as fire is a prevalent disturbance agent in this ecosystem (Stringham et al. 2003; Lund 2007; Abatzoglou and Kolden, 2011). Additionally, species shifts (i.e. the replacement of native species with invasive species) provide a unique opportunity to study how biomass burning emissions are affected by large-scale species migrations (Figure 2).

Three ecoregions in the northern Great Basin, U.S. were chosen as study sites to represent temperate shrub-steppe ecosystems. The Columbia Plateau, Northern Great Basin and Range, and Central Basin and Range ecoregions all incorporate shrub-steppe ecosystems in varying degrees of invasive plant invasion.

To examine the burned area mapping uncertainties we selected four shrub-steppe fires that burned in the summer of 2006 and 2009 in the Great Basin, United States. The fires all burned in similar Great Basin vegetation types characterized by patchy sagebrush (*Artemisia* spp.), bunchgrasses, and annual invasive grasses, including cheatgrass (*Bromus tectorum* L.) and were selected as they visually exhibited different degrees of within-fire patch heterogeneity. Due to logistics of transporting collected samples, all fuels burned in this study were collected at the Columbia National Wildlife Refuge, WA, located at 46.965°N - 119.251°W in the Columbia Plateau ecoregion. The collection site had uniform topography (elevation range: 290-300m) and a fairly uniform species distribution of Wyoming big sagebrush (*Artemisia tridentata* Nutt. ssp. *wyomingensis* Beetle and Young), bluebunch wheatgrass (*Pseudoroegneria spicata* Pursh), and cheatgrass.

Scope and Objectives

The goal of this work was to increase our understanding of burned area and emission factors from wildfires in shrub-steppe ecosystems. Figure 3 presents the direction of research included in this thesis and future work. It was not the intent of this work to estimate emission flux for shrub-steppe ecosystems, but rather to examine the sources of uncertainty with two of its components: area burned (A) and emission factors (EF_x). The emissions work in this thesis is limited to 1) three rangeland species, and 2) four common trace gases.

The main objectives of this work were to 1) test the accuracy of the MTBS fire perimeter product for large shrub-steppe fires, 2) investigate the most accurate area burned method using moderate spatial resolution data (Landsat TM), 3) assess the effects of seasonality (moisture content and phenology) on emission factors of common trace gases emitted during the combustion of three rangeland plant species.

Chapter Summaries

The research within this thesis focuses on quantifying the uncertainty involved with key terms in the emission flux calculation and are formatted according to the manuscript structure required for each journal:

Chapter 2 examines the accuracy of the Monitoring Trends in Burn Severity (MTBS), in addition to several other spectral indices, for mapping area burned in shrub-steppe ecosystems. Area burned was investigated as it is a significant component of both emissions calculations and modeling trends in area burned. Chapter 2 has been accepted for publication by the *International Journal of Wildland Fire* with Luigi Boschetti, Wade Tinkham, Alistair Smith, Karen Lannom, and Beth Newingham (Sparks et al., in press).

Chapter 3 is an exploration into seasonal influences on major carbon and nitrogen trace gas emissions from sagebrush-steppe fires. Specifically, this chapter details how seasonal changes in plant phenology and moisture content affect the production of CO₂, CO, NO, and NO₂ emission factors.

Following initiation of this thesis, it became apparent that the scope was too large and thus this thesis focuses on only the area burned and the sagebrush emission factors. Additional work conducted during this thesis is contained within the appendices:

Appendix A details the emission factor results of the grasses burned in this study. These data will be additionally analyzed beyond the lifetime of this thesis and are being prepared for an article within the *Journal of Geophysical Research*.

Appendix B details preliminary research to characterize the role of fuel moisture content on combustion completeness and fire radiative energy retrievals. This appendix represented a team effort and was published in 2013 in *Geophysical Research Letters* with Alistair Smith, Wade Tinkham, David Roy, Luigi Boschetti, Robert Kremens, Sanath Kumar, and Michael Falkowski.

References

- Abatzagluo, J.T., and Kolden, C.A. (2011). Climate change in western US deserts: Potential for increased wildfire and invasive annual grasses. *Rangeland Ecology and Management*, 64(5), 471-478.
- Akagi, S. K., Yokelson, R. J., Wiedinmyer, C., Alvarado, M. J., Reid, J. S., Karl, T., Crouse, J. D., and Wennberg, P. O. (2011). Emission factors for open and domestic biomass burning for use in atmospheric models. *Atmospheric Chemistry and Physics*, 11, 4039-4072.
- Amiro, B. D., Todd, J. B., Wotton, B. M., Logan, K. A., Flannigan, M. D., Stocks, B. J., Mason, J. A., Martell, D. L. and Hirsch, K. G. (2001). Direct carbon emissions from Canadian forest fires, 1959-1999. *Canadian Journal of Forest Research*, 31, 512-525.
- Andreae, M. O., and P. Merlet (2001), Emission of trace gases and aerosols from biomass burning, *Global Biogeochemical Cycles*, 15(4), 955-966.
- Bertschi, I., Yokelson, R. J., Ward, D. E., Babbitt, R. E., Susott, R. A., Goode, J. G., and Hao, W. M. (2003). Trace gas and particle emissions from fires in large diameter and belowground biomass fuels. *Journal of Geophysical Research*, 108, doi:10.1029/2002JD002100.
- Burling, I. R., Yokelson, R. J., Griffith, D. W., Johnson, T. J., Veres, P., Roberts, J., Warneke, C., Urbanski, S. P., Reardon, J., Weise, D. R., Hao, W. M., and De Gouw, J. A. (2010). Laboratory measurements of trace gas emissions from biomass burning of fuel types from the southeastern and southwestern United States. *Atmospheric Chemistry and Physics*, 10(22), 11115-11130.
- Burling, I. R., Yokelson, R. J., Akagi, S. K., Urbanski, S. P., Wold, C. E., Griffith D. W. T., Johnson, T. J., Reardon, J., and Weise, D. R. (2011). Airborne and ground-based measurements of the trace gases and particles emitted by prescribed fires in the United States. *Atmospheric Chemistry and Physics*, 11, 12197-12216.
- Cahoon, D. R., Stocks, B. J., Levine, J. S., Cofer III, W. R., and Barber, J. A. (1996). Monitoring the 1992 forest fires in the boreal ecosystem using NOAA AVHRR satellite imagery, in *Biomass Burning and Climate Change. Vol 2. Biomass burning in South America, Southeast Asia, and Temperate and Boreal Ecosystems, and the Oil Fires of Kuwait*, edited by J.S. Levine, pp. 795-802, MIT Press, Cambridge, MA.
- Chen, L. W. A., Moosmuller, H., Arnott, W. P., Chow, J. C., Watson, J. G., Susott, R. A., Babbitt, R. E., Wold, C. E., Lincoln, E. N., and Hao, W. M. (2007). Emissions from laboratory combustion of wildland fuels: emission factors and source profiles. *Environmental Science and Technology*, 41, 4317-4325.
- Christian, T. J., Kleiss, B., Yokelson, R. J., Holzinger, R., Crutzen, P. J., Hao, W. M., Saharjo, B. H., and Ward, D. E. (2003). Comprehensive laboratory measurements of

- biomass-burning emissions: 1. Emissions from Indonesian, African, and other fuels. *Journal of Geophysical Research*, 108, doi:10.1029/2003JD003704.
- Cofer, W. R., Levine, J. S., Sebacher, D. I., Winstead, E. L., Riggan, P. J., Stocks, B. J., Brass, J. A., Ambrosia, V. G., and Boston, P. J. (1989). Trace gas emissions from chaparral and boreal forest fires. *Journal of Geophysical Research*, 94, 2255-2259.
- Cofer, W. R., Levine, J. S., Winstead, E. L., Cahoon, D. R., Sebacher, D. I., Pinto, J. P., and Stocks, B. J. (1996). Source compositions of trace gases released during African savanna fires. *Journal of Geophysical Research*, 101, 23597-23602.
- Cofer, W. R., Winstead, E. L., Stocks, B. J., Overbay, L. W., Goldammer, J. G., Cahoon, D. R., and Levine, J. S. (1996). Emissions from boreal forest fires: are the atmospheric impacts underestimated? In *Biomass Burning and Climate Change. Vol 2. Biomass burning in South America, Southeast Asia, and Temperate and Boreal Ecosystems, and the Oil Fires of Kuwait*, edited by J.S. Levine, pp. 834-839, MIT Press, Cambridge, MA.
- Cofer, W. R., Winstead, E. L., Stocks, B. J., Goldammer, J. G., and Cahoon, D. R. (1998). Crown fire emissions of CO₂, CO, H₂, CH₄, and TNMHC from a dense jack pine boreal forest fire. *Geophysical Research Letters*, 25(21), 3919-3922.
- Conard, S. G., Sukhinin, A. I., Stocks, B. J., Cahoon, D. R., Davidenko, E. P., and Ivanova, G. A. (2002). Determining effects of area burned and fire severity on carbon cycling and emissions in Siberia. *Climatic Change*, 55, 197-211.
- Dixon, R. K., Brown, S., Houghton, R. A., Solomon, A. M., Trexler, M. C., and Wisniewski, J. (1994). Carbon pools and flux of global forest ecosystems. *Science*, 263, 185-190.
- Fearnside, P. M., Leal, Jr., N., and Fernandes, F. M. (1993). Rainforest burning and the global carbon budget: biomass, combustion efficiency, and charcoal formation in the Brazilian Amazon. *Journal of Geophysical Research*, 98, 16733-16743.
- Ferek, R. J., Reid, J. S., Hobbs, P. V., Blake, D. R., and Liousse, C. (1998). Emission factors of hydrocarbons, halocarbons, trace gases and particles from biomass burning in Brazil. *Journal of Geophysical Research*, 103, 32107-32118.
- Freeborn, P. H., Wooster, M. J., Hao, W. M., Ryan, C. A., Nordgren, B. L., Baker, S. P., and Ichoku, C. (2008). Relationships between energy release, fuel mass loss, and trace gas and aerosol emissions during laboratory biomass fires. *Journal of Geophysical Research*, 113, D01301, doi:10.1029/2007JD008679.
- French, N. H. F., Goovaerts, P., and Kasischke, E.S. (2004). Uncertainty in estimating carbon emissions from boreal forest fires. *Journal of Geophysical Research*, 109, D14S08.

- Goode, J. G., Yokelson, R. J., Susott, R. A., and Ward, D. E. (1999). Trace gas emissions from laboratory biomass fires measured by open-path Fourier transform infrared spectroscopy: Fires in grass and surface fuels. *Journal of Geophysical Research*, *104*, 21237-21245.
- Goode, J. G., Yokelson, R. J., Ward, D. E., Susott, R. A., Babbitt, R. E., Davies, M. A., and Hao, W. M. (2000). Measurements of excess O₃, CO₂, CO, CH₄, C₂H₄, C₂H₂, HCN, NO, NH₃, HCOOH, CH₃COOH, HCHO, and CH₃OH in 1997 Alaskan biomass burning plumes by airborne Fourier transform infrared spectroscopy (AFTIR). *Journal of Geophysical Research*, *105*, 22147-22166.
- Hao, W. M., Liu, M. H., and Crutzen, P. J. (1990). Estimates of annual and regional releases of CO₂ and other trace gases to the atmosphere from fires in the tropics, based on the FAO statistics for the period 1975-1980, in *Fire in the Tropical Biota, Ecol. Stud.*, vol. 84, edited by J.G. Goldammer, pp.440-462, Springer, New York.
- Hao, W. M. and Ward, D. E. (1993). Methane production from global biomass burning. *Journal of Geophysical Research*, *98*, 20657-20661.
- Hao, W. M. and Liu, M. (1994). Spatial and temporal distribution of tropical biomass burning. *Global Biogeochemical Cycles*, *8*, 495-503.
- Hegg, D. A., Radke, L. F., Hobbs, P. V., Rasmussen, R. A., and Riggan, P. J. (1990). Emissions of some trace gases from biomass fires. *Journal of Geophysical Research*, *95*, 5669-5675.
- Hoffa, E. A, Ward, D. E., Hao, W. M., Susott, R. A., and Wakimoto, R. H. (1999). Seasonality of carbon emissions from biomass burning in a Zambian savanna. *Journal of Geophysical Research*, *104*(11), 13841-13853.
- Hurst, D. F., Griffith, D. W., Carras, J. N., Williams, D. J., and Fraser, P. J. (1994). Measurements of trace gases emitted by Australian savanna fires during the 1990 dry season. *Journal of Atmospheric Chemistry*, *18*, 33-56.
- Isaev, A. S., Korovin, G. N., Bartalev, S. A., Ershov, D. V., Janetos, A., Kasischke, E. S., Shugart, H. H., French, N. H. F., Orlick, B. E., and Murphy, T. L. (2002). Using remote sensing to assess Russian forest fire carbon emissions. *Climatic Change*, *55*, 235-249.
- Intergovernmental Panel on Climate Change (IPCC) (2013). *Climate Change 2013: The Physical Science Basis*. Cambridge University Press, Cambridge, UK.
- Jacobson, M. Z. (2001b). Strong radiative heating due to the mixing state of black carbon in atmospheric aerosols. *Nature*, *409*, 695-697.

- Jones, B. M., Kolden, C. A., Jandt, R., Abatzoglou, J. T., Urban, F., and Arp, C. D. (2009). Fire behavior, weather, and burn severity of the 2007 Anaktuvuk River tundra fire, North Slope, Alaska. *Arctic, Antarctic, and Alpine Research*, *41*, 309-316.
- Justice, C. O., Giglio, L., Korontzi, S., Owens, J., Morisette, J. T., Roy, D., Descloitres, J., Alleaume, S., Petitcolin, F., and Kaufman, Y. (2002). The MODIS fire products. *Remote Sensing of Environment*, *83*, 244-262.
- Kasischke, E. S., and French, N. H. (1995). Locating and estimating the areal extent of wildfires in Alaskan boreal forests using multiple-season AVHRR NDVI composite data. *Remote Sensing of Environment*, *51*(2), 263-275.
- Kasischke, E. S., Christensen, N. L., Jr., Stocks, B. J. (1995). Fire, global warming, and the carbon balance of boreal forests. *Ecological Applications*, *5*(2), 437-451.
- Kasischke, E. S., Bergen, K., Fennimore, R., Sotelo, F., Stephens, G., Janetos, A., and Shugart, H. H. (1999). Satellite imagery gives a clear picture of Russia's boreal forest fires. *EOS Transactions American Geophysical Union*, *80*, 141-147.
- Kasischke, E. S., and Bruhwiler, L. P. (2003). Emissions of carbon dioxide, carbon monoxide, and methane from boreal forest fires in 1998. *Journal of Geophysical Research*, *108*, 8146, doi:10.1029/2001JD000461.
- Kasischke, E. S., O'Neill, K. P., French, N. H. F., and Bourgeau-Chavez, L. L. (2000). Controls on patterns of biomass burning in Alaskan boreal forests, in *Fire, Climate Change, and Carbon Cycling in the Boreal Forest*, edited by E. S. Kasischke and B. J. Stocks, pp. 173-196, Springer, New York.
- Kaufman, Y. J., Setzer, A., Ward, D., Tanre, D., Holben, B. N., Menzel, P., Pereira, M. C., and Rasmussen, R. (1992). Biomass Burning Airborne and Spaceborne Experiment in the Amazonas (BASE-A). *Journal of Geophysical Research*, *97*, 14581-14599.
- Keene, W. C., Lobert, J. M., Crutzen, P. J., Maben, J. R., Scharffe, D. H., Landmann, T., Hely, C., and Brain, C. (2006). Emissions of major gaseous and particulate species during experimental burns of southern African biomass. *Journal of Geophysical Research*, *111*, D04301, doi:10.1029/2005JD006319.
- Keyser, A. R., Kimball, J. S., Nemani, R. R., and Running, S. W. (2000). Simulating the effects of climate change on the carbon balance of North America high-latitude forests. *Global Change Biology*, *6*, 185-195.
- Khalil, M. A. K., and Rasmussen, R. A. (1988). Carbon monoxide in the Earth's atmosphere: indications of a global increase. *Nature*, *332*, 242-245.
- Korontzi, S., Ward, D. E., Susott, R. A., Yokelson, R. J., Justice, C. O., Hobbs, P. V., Smithwick, E. A. H., and Hao, W. M. (2003). Seasonal variation and ecosystem

- dependence of emission factors for selected trace gases and PM_{2.5} for southern African savanna fires. *Journal of Geophysical Research: Atmospheres* (1984–2012), 108(D24).
- Lashof, D. A., and Ahuja, D. R. (1990). Relative contributions of greenhouse gas emissions to global warming. *Nature*, 344, 529-531.
- Laursen, K. K., Hobbs, P. V., Radke, L. F., and Rasmussen, R. A. (1992). Some trace gas emissions from North American biomass fires with an assessment of regional and global fluxes from biomass burning. *Journal of Geophysical Research*, 97, 20687-20701.
- Lentile, L.B., Holden, Z.A., Smith, A.M.S., Falkowski, M.J., Hudak, A.T., Morgan, P., Lewis, S.A., Gessler, P.E., Benson, N.C. (2006). Remote sensing techniques to assess active fire characteristics and post-fire effects, *International Journal of Wildland Fire* 15, 3, 319-345, doi: 10.1071/WF05097.
- Levine, J. S. and Cofer III, W. R. (2000). Boreal forest fire emissions and the chemistry of the atmosphere, in *Fire, Climate Change, and Carbon Cycling in the Boreal Forest*, edited by E.S. Kasischke and B.J. Stocks, pp.31-48, Springer, New York.
- Liu, Y. (2004). Variability of wildland fire emissions across the contiguous United States. *Atmospheric Environment*, 38, 3489-3499.
- Lund, G.H. (2007). Accounting for the world's rangelands. *Rangelands*, 2, 3–10.
- Nance, J. D., Hobbs, P. V., Radke, L. W., and Ward, D. E. (1993). Airborne measurements of gases and particles from an Alaskan wildfire. *Journal of Geophysical Research*, 98, 14873-14882.
- Pereira, J.M.C., Sá, A.C.L., Sousa, A.M.O., Silva, J.M.N., Santos, T.N., Carreiras, J.M.B. (1999). Spectral characterization and discrimination of burnt areas. In *Remote Sensing of Large Wildfires in the European Mediterranean Basin*, pp.123-138 (E. Chuvieco, ed), Springer-Verlag, Berlin.
- Reisen, F., Meyer, C. P., McCaw, L., Powell, J. C., Tolhurst, K., Keywood, M. D., and Gras, J. L. (2011). Impact of smoke from biomass burning on air quality in rural communities in southern Australia. *Atmospheric Environment*, 45, 3944-3953.
- Roy, D.P., Jin, Y., Lewis, P.E., Justice, C.O. (2005). Prototyping a global algorithm for systematic fire-affected area mapping using MODIS time series data. *Remote Sensing of Environment*, 97, 137-162.
- Roy, D.P., Boschetti, L., Justice, C.O., Ju, J. (2008). The Collection 5 MODIS Burned Area Product - Global Evaluation by Comparison with the MODIS Active Fire Product. *Remote Sensing of Environment*, 112, 3690-3707.

- Running, S. W., Justice, C. O., Salomonson, V., Hall, D., Barker, J., Kaufmann, Y. J., Strahler, A. H., Huete, A. R., Muller, J. P., Vanderbilt, V., Wan, Z. M., Teillet, P., and Carneggie, D. (1994). Terrestrial remote sensing science and algorithms planned for EOS/MODIS. *International Journal of Remote Sensing*, *15*, 3587-3620.
- Scholes, R. J., Kendall, J., and Justice, C. O. (1996). The quantity of biomass burned in southern Africa. *Journal of Geophysical Research*, *101*(19), 23667-23676.
- Scholes, R.J., Ward, D.E., and Justice, C.O. (1996). Emissions of trace gases and aerosol particles due to vegetation burning in southern hemisphere Africa. *Journal of Geophysical Research*, *101*(19), 23677-23682.
- Simpson, I. J., Akagi, S. K., Barletta, B., Blake, N. J., Choi, Y., Diskin, G. S., Fried, A., Fuelberg, H. E., Meinardi, S., Rowland, F. S., Vay, S. A., Weinheimer, A. J., Wennberg, P. O., Wiebring, P., Wisthaler, A., Yang, M., Yokelson, R. J., and Blake, D. R. (2011). Boreal forest fire emissions in fresh Canadian smoke plumes: C1-C10 volatile organic compounds (VOCs), CO₂, CO, NO₂, NO, HCN and CH₃CN. *Atmospheric Chemistry and Physics*, *11*, 6445-6463.
- Sinha, P., Hobbs, P. V., Yokelson, R. J., Bertschi, I. T., Blake, D. R., Simpson, I. J., Gao, S., Kirchstetter, T. W., and Novakov, T. (2003). Emissions of trace gases and particles from savanna fires in southern Africa. *Journal of Geophysical Research*, *108*, D13, 8487, doi:10.1029/2002JD002325.
- Seiler, W., and Crutzen, P. J. (1980). Estimates of gross and net fluxes of carbon between the biosphere and the atmosphere from biomass burning. *Climatic change*, *2*(3), 207-247.
- Sinha, P., Hobbs, P. V., Yokelson, R. J., Blake, D. R., Gao, S., and Kirchstetter, T. W. (2004). Emissions from miombo woodland and dambo grassland savanna fires. *Journal of Geophysical Research*, *109*, D11305, doi:10.1029/2004JD004521.
- Smith, A.M.S, Tinkham, W. T., Roy, D. P., Boschetti, L., Kremens, R. L., Kumar, S. S., Sparks, A. M., and Falkowski, M. J. (2013). Quantification of fuel moisture effects on biomass consumed derived from fire radiative energy retrievals. *Geophysical Research Letters*, *40*(23), 6298-6302.
- Sparks, A.M., Boschetti, L., Smith, A.M.S., Tinkham, W.T., Lannom, K.O., and Newingham, B. (in press). An accuracy assessment of the MTBS burned area products for shrub-steppe fires in the northern Great Basin, United States. *International Journal of Wildland Fire*.
- Stringham, T.K., Kruger, W.C., and Shaver, P.L. (2003). State and transition modeling: An ecological process approach. *Journal of Range Management*, *56*(2), 106-113, doi: 10.2307/4003893.

- Urbanski, S. P., Hao, W. M., Baker, S. (2009). Chapter 4 Chemical composition of wildland fire emissions, in *Developments in Environmental Science, Volume 8*, edited by A. Bytnerowicz, M. Arbaugh, A. Riebau, and C. Andersen, pp. 79-107, Elsevier, ISSN:1474-8177/DOI:10.1016/S1474-8177(08)00004-1.
- van der Werf, G. R., Randerson, J. T., Giglio, L., Collatz, G. J., Mu, M., Kasibhatla, P. S., Morton, D. C., DeFries, R. S., Jin, Y., and van Leeuwen, T. T. (2010). Global fire emissions and the contribution of deforestation, savanna, forest, agricultural, and peat fires (1997-2009). *Atmospheric Chemistry and Physics*, 10, 11707-11735.
- Ward, D.E. (1979). Particulate matter and aromatic hydrocarbon emissions from the controlled combustion of alpha-pinene. Dissertation, University of Washington, Seattle, WA, 244p.
- Ward, D. E., Susott, R. A., Kauffman, J. B., Babbitt, R. E., Cummings, D. L., Dias, B., Holben, B. N., Kaufman, Y. J., Rasmussen, R. A., and Setzer, A. W. (1992). Smoke and fire characteristics for Cerrado and deforestation burns in Brazil: BASE-B Experiment. *Journal of Geophysical Research*, 97, 14601-14619.
- Ward, D. E., Hao, W. M., Susott, R. A., Babbitt, R. E., Shea, R. W., Kauffman, J. B. and Justice, C. O. (1996). Effect of fuel composition on combustion efficiency and emission factors for African savanna ecosystems. *Journal of Geophysical Research*, 101, 23569-23576.
- Wiedinmyer, C., and Hurteau, M. D. (2010). Prescribed fire as a means of reducing forest carbon emissions in the western United States. *Environmental Science and Technology*, 44, 1926-1932.
- Wiedinmyer, C., Akagi, S. K., Yokelson, R. J., Emmons, L. K., Al-Saadi, J. A., Orlando, J. J., and Soja, A. J. (2011). The Fire INventory from NCAR (FINN): a high resolution global model to estimate the emissions from open burning. *Geoscientific Model Development*, 4, 625-641, doi:10.5194/gmd-4-625-2011.
- Yokelson, R. J., Goode, J. G., Ward, D. E., Susott, R. A., Babbitt, R. E., Wade, D. D., Bertschi, I., Griffith, D. W. T., and Hao, W. M. (1999). Emissions of formaldehyde, acetic acid, methanol, and other trace gases from biomass fires in North Carolina measured by airborne Fourier transform infrared spectroscopy. *Journal of Geophysical Research*, 104, 30109-30125.
- Yokelson, R. J., Bertschi, I. T., Christian, T. J., Hobbs, P. V., Ward, D. E., and Hao, W. M. (2003). Trace gas measurements in nascent, aged, and cloud-processed smoke from African savanna fires by airborne Fourier transform infrared spectroscopy (AFTIR). *Journal of Geophysical Research*, 108, doi:10.1029/2002JD002322.
- Yokelson, R. J., Karl, T., Artaxo, P., Blake, D. R., Christian, T. J., Griffith, D. W. T., Guenther, A., and Hao, W. M. (2007). The tropical forest and fire emissions experiment:

overview and airborne fire emission factor measurements. *Atmospheric Chemistry and Physics*, 7, 5175-5196.

Yokelson, R. J., Christian, T. J., Karl, T. G., and Guenther, A. (2008). The tropical forest and fire emissions experiment: laboratory fire measurements and synthesis of campaign data. *Atmospheric Chemistry and Physics*, 8, 3509-3527.

Yokelson, R. J., Burling, I. R., Urbanski, S. P., Atlas, E. L., Adachi, K., Buseck, P. R., Wiedinmyer, C., Akagi, S. K., Toohey, D. W., and Wold, C. E. (2011). Trace gas and particle emissions from open biomass burning in Mexico. *Atmospheric Chemistry and Physics*, 11, 6787-6808.

Yokelson, R. J., Burling, I. R., Gilman, J. B., Warneke, C., Stockwell, C. E., Gouw, J. D., Akagi, S. K., Urbanski, S. P., Veres, P., Roberts, J. M., Kuster, W. C., Reardon, J., Griffith, D. W. T., Johnson, T. J., Hosseini, S., Miller, J. W., Cocker III, D. R., Jung, H., and Weise, D. R. (2013). Coupling field and laboratory measurements to estimate the emission factors of identified and unidentified trace gases for prescribed fires. *Atmospheric Chemistry and Physics*, 13, 89-116.

Table 1. Common spectral indices used for burned area mapping.

Index	Equation	Reference
NDVI	$(\rho_{\text{NIR}} - \rho_r) / (\rho_{\text{NIR}} + \rho_r)$	Rouse et al. (1974)
NBR	$(\rho_{\text{NIR}} - \rho_{\text{SWIR}}) / (\rho_{\text{NIR}} + \rho_{\text{SWIR}})$	Lopez-Garcia and Caselles (1991)
MIRBI	$10\rho_{\text{SWIR}} - 9.8\rho_{\text{LNIR}} + 2$	Trigg and Flasse (2001)
CSI	$\rho_{\text{NIR}} / \rho_{\text{LNIR}}$	Smith et al. (2005b)
BAI	$[(G_r - \rho_r)^2 + (G_{\text{NIR}} + \rho_{\text{NIR}})^2]^{-1}$	Chuvieco et al. (2002)

ρ_r = sensor red reflectance (TM band 3)

G_r = ground measured red reflectance

ρ_{NIR} = sensor NIR reflectance (TM band 4)

G_{NIR} = ground measured NIR reflectance

ρ_{LNIR} = sensor long NIR reflectance (TM band 5)

ρ_{SWIR} = sensor SWIR reflectance (TM band 7)

Table 2. Average emission factors of major carbonaceous and nitrogenous trace gas species and PM_{2.5} for savanna, tropical forest, boreal, and temperate biomes.

Species	Savanna ^a	Tropical Forest ^b	Boreal ^c	Temperate ^d
CO ₂	1706 (±6)	1585 (±5)	1526 (±4)	1672 (±5)
CO	71 (±32)	116 (±35)	133 (±28)	89 (±26)
CH ₄	1.95 (±57)	6.2 (±38)	4.76 (±41)	4.36 (±49)
NMHC	2.62 (±44)	6.5 (±47)	3.3 (±63)	1.85 (±25)
NO _x	2.87 (±32)	1.46 (±55)	1.51 (±36)	4.36 (±33)
N ₂ O	-	-	0.29 (±77)	0.31 (±228)
PM _{2.5}	5.6 (±48)	9.64 (±48)	10.1 (±84)	11.27 (±42)

Emission factors are reported in g kg⁻¹ (± CV).

^aData sources are: *Cofer et al.* [1996], *Ferek et al.* [1998], *Freeborn et al.* [2008], *Hao and Ward* [1993], *Hurst et al.* [1994a], *Kaufman et al.* [1992], *Keene et al.* [2006], *Korontzi et al.* [2004], *Sinha et al.* [2003, 2004], *Ward et al.* [1992, 1996], *Yokelson et al.* [2003].

^bData sources are: *Christian et al.* [2003, 2007], *Ferek et al.* [1998], *Kaufman et al.* [1992], *Ward et al.* [1992], *Yokelson et al.* [2007, 2008].

^cData sources are: *Bertschi et al.* [2003], *Cofer et al.* [1996, 1998], *French et al.* [2004], *Goode et al.* [2000], *Hegg et al.* [1990], *Kasichke and Bruhwiler* [2003], *Laursen et al.* [1992], *Nance et al.* [1993], *Simpson et al.* [2011], *Susott et al.* [1991], *Urbanski et al.* [2009].

^dData sources are: *Bertschi et al.* [2003], *Burling et al.* [2010, 2011], *Freeborn et al.* [2008], *Friedli et al.* [2001], *Hegg et al.* [1990], *Laursen et al.* [1992], *Urbanski et al.* [2009], *Yokelson et al.* [1996, 1999, 2011].

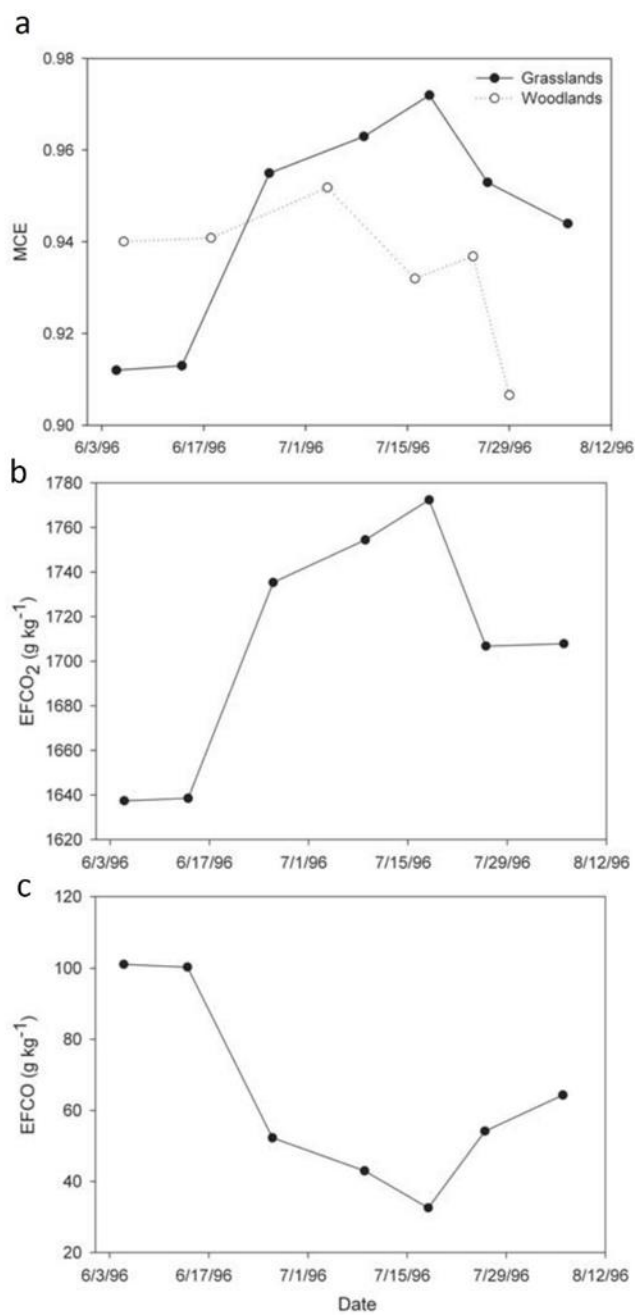


Figure 1. Seasonal dependence of a) Modified combustion efficiency for African grassland and woodland fires, b) EF_{CO_2} from grassland fires, and c) EF_{CO} from grassland fires (Image Source: Korontzi et al. [2003]).

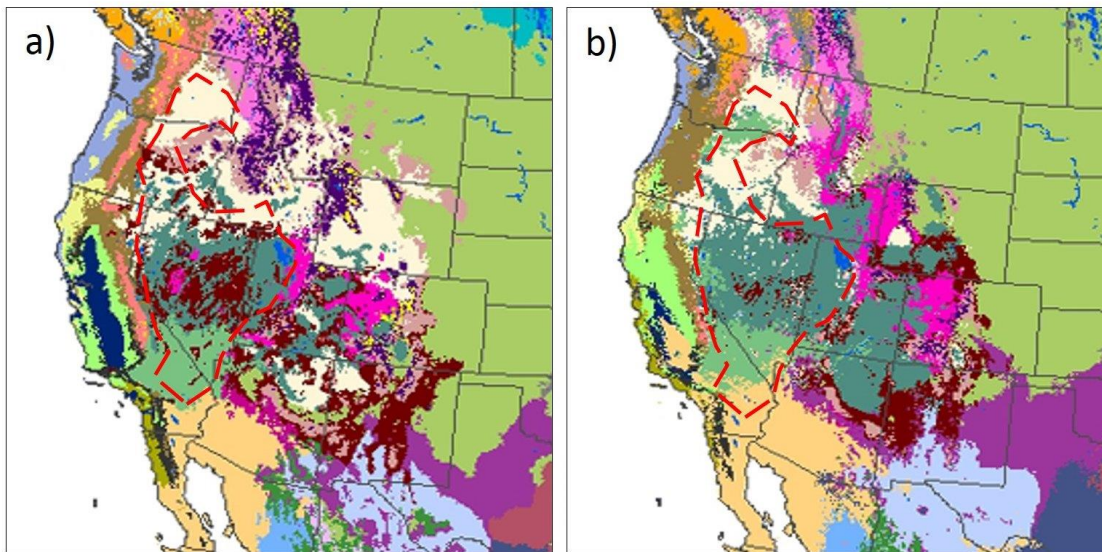


Figure 2. Predicted North American biome distribution shifts from, a) present day to, b) year2090 (adapted from Rehfeldt et al. [2012]). Red outline is approximate boundary of Great Basin region. Great Basin region biomes: white = Great Basin shrub-grassland, dull purple = Rocky Mountain montane conifer forest, dark red = Great Basin conifer woodland, dark teal = Great Basin desert scrub, pink = Great Basin montane scrub, light teal = Mohave desert scrub, tan = Sonoran desert scrub.

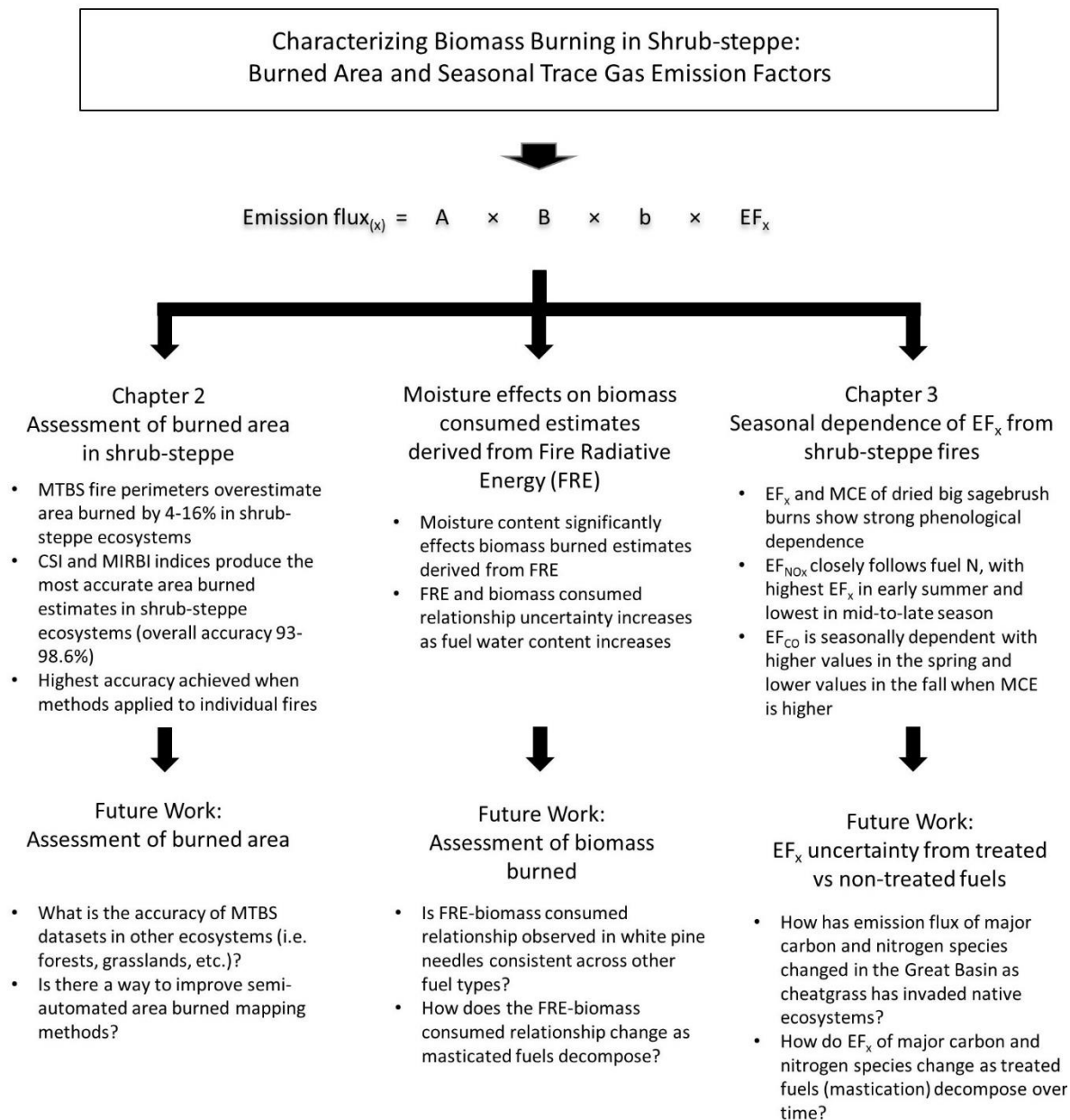


Figure 3. Progression of thesis research and future work avenues.

Chapter 2

An Accuracy Assessment of the MTBS Burned Area Product for Shrub-steppe Fires in the Northern Great Basin, United States

Abstract

Although fire is a common disturbance in shrub-steppe, few studies have specifically tested burned area mapping accuracy in these semi-arid to arid environments. We conducted a preliminary assessment of the accuracy of the Monitoring Trends in Burn Severity (MTBS) burned area product on four shrub-steppe fires that exhibited varying degrees of within-fire patch heterogeneity. Independent burned area perimeters were derived through visual interpretation and were used to cross-compare the MTBS burned area perimeters with classifications produced using set thresholds on the Relativized differenced Normalized Burn Index (RdNBR), mid-infrared burn index (MIRBI), and the char soil index (CSI). Overall, CSI provided the most consistent accuracies (96.3-98.6%), with only small commission errors (1.5-4.43%). MIRBI also had relatively high accuracies (92.9-97.9%) and small commission errors (2.1-10.8%). The MTBS burned area product had high commission errors (4.3-15.5%), primarily due to inclusion of unburned islands and fingers within the fire perimeter. The RdNBR burned area maps exhibited very high commission errors (17.2-42.4%), however, when constrained by the MTBS perimeter provided accuracies (93.1-97.4%) comparable to CSI and MIRBI. Studies seeking to use MTBS data to analyze trends in burned area should apply spectral-indices to constrain the final burned area maps.

Introduction

Shrub-steppes are semi-arid to arid lands that are dominated by shrubs with intermixed grasses and forbs and are sustained through ecological processes such as fire, drought, and species succession, among others (Stringham *et al.* 2003; Lund 2007; Abatzoglou and Kolden, 2011). While fire is an important disturbance agent in North American shrub-steppe systems, its historic prevalence has been less than in forests due to low plant cover and thus gaps in continuous surface vegetation to carry fire (West and Young 2000). Steppe fires can alter nutrient availability, promote the establishment of seral species, and alter wildlife habitats (Crawford *et al.* 2004; Chambers *et al.* 2007). Area burned assessments in these

ecosystems are necessary such that land management personnel can effectively target and allocate resources to rehabilitation and restoration efforts (Baker 2006). We recognize that moderate spatial resolution sensors (e.g., MODIS: 0.25-1.0 km pixels) may continue to be used for global area burned mapping assessments (Roy *et al.* 2008); however, high spatial resolution datasets (i.e. Landsat-type sensors: 30m pixels) will likely remain the most commonly applied by land and fire management personnel due to the spatial detail they provide (Lentile *et al.* 2006).

The Monitoring Trends in Burn Severity (MTBS) project was initiated with the objective of producing systematic, multiyear burned area maps and associated burn severity information over the United States, with a primary focus on land management support (Eidenshink *et al.* 2007). The product is generated with a semi-automated process, but limited validation of the MTBS maps, or similar perimeters have been presented in the literature (Brewer *et al.*, 2005; Sunderman and Weisberg, 2011; Kolden *et al.*, 2012). However, accuracy assessment of the MTBS maps is essential given these data have been widely used for the characterization of area burned and temporal analysis of regional area burned trends (Dillon *et al.* 2011; Zheng *et al.*, 2011; Morton *et al.* 2012; Randerson *et al.*, 2012; Riley *et al.* 2013; Lannom *et al.* 2014). The objective of this study was to conduct a comparative assessment of the semi-automated area burned maps produced by the MTBS project as applied to shrub-steppe fires. The specific questions we sought to address for the MTBS area burned product were:

- (1) What is the areal accuracy of the burned area MTBS polygons?
- (2) Can the accuracy be improved by applying a simple threshold to spectral indices within the polygons?

Datasets

Study Area and Imagery

For this preliminary study, we selected four shrub-steppe fires that burned in the summer of 2006 and 2009 in the Great Basin, United States (Figure 1). The fires all burned in similar Great Basin vegetation types characterized by patchy sagebrush (*Artemisia* spp.), bunchgrasses, and annual invasive grasses, including cheatgrass (*Bromus tectorum*). The Burnt Fire burned mostly in the sagebrush and grass vegetation on the edge of the Black

Pine Mountains of Idaho and expanded to several adjacent agriculture fields. The Hogups and Scorpio fires burned in grass and sagebrush vegetation in the Hogups Mountains northeast of the Great Salt Lake, Utah. The Dry Creek Complex fire burned mostly in grass and sagebrush near the Columbia River six miles north of Sunnyside, WA. The four fires were selected as they visually exhibited different degrees of within-fire patch heterogeneity. The Scorpio fire consisted of large tracts of area burned with few unburned patches, whereas the Hogups and Dry Creek Complex fires contained many unburned islands within the perimeter, as well as numerous burned “fingers” that extend from the main body of area burned. The Burnt fire represents the intermediate scenario, with a small number of unburned patches.

The fires are covered by Landsat path 39 row 31 (Burnt, Hogups, and Scorpio fires) and Landsat path 45 row 28 (Dry Creek Complex). Landsat 5 TM imagery was selected, because since 2003, Landsat 7 ETM+ images are affected by the failure of the Scan Line Corrector (SLC) and are unsuitable for mapping ephemeral landcover changes, such as fires. The selected Landsat 5 images were acquired on July 15th, 2006 (Scorpio), August 16th, 2006 (Burnt and Hogups), and October 5th, 2009 (Dry Creek Complex). Calibration and atmospheric correction for each scene was performed using the Landsat Ecosystem Disturbance Adaptive Processing Systems (LEDAPS) (Masek *et al.* 2006, 2008). The images were sub-set to the minimum enclosing rectangle around each fire.

We acquired also post-fire aerial imagery from the National Agriculture Imagery Program (NAIP) for the Burnt (21st July 2006), Scorpio (27th August 2006), and Hogups (27th August 2006). No NAIP data was available for the Dry Creek 2009 fire. NAIP imagery consists of orthorectified visible (red, green, blue) un-calibrated digital aerial photographs with spatial resolution of 1m (Scorpio and Hogups) or 2 m (Burnt).

MTBS Products

The MTBS project develops area burned and severity maps across all lands of the United States from 1984 onwards, using Landsat imagery. All fires larger than ~2 km² (500 acres) are mapped in the Eastern United States and ~4 km² (1000 acres) in the western United States. The available products include:

- Fire perimeters, distributed in vector format (ESRI shapefile)

- Pre-fire and Post-fire Landsat TM/ETM+ raster images, clipped to a 3 km buffered box around each fire perimeter
- NBR, dNBR and RdNBR spectra index rasters, clipped to a 3 km buffered box around each fire perimeter
- Thematic burn severity map, with 5 severity classes, defined for each pixel within a fire perimeter

In the present study we used two of the MTBS products: the fire perimeters and the RdNBR images. The fire perimeters are defined by analysts who rapidly and manually digitize the Landsat imagery. The polygons exhibit a degree of simplification of the fire perimeter and, by project requirement, do not identify any unburned islands within the perimeter. RdNBR was developed by Miller and Thode (2007) as a version of dNBR that normalizes for the pre-fire vegetation. $RdNBR = dNBR \div \sqrt{(NBR_{prefire}/1000)}$, $dNBR = NBR_{pre} - NBR_{post}$, $NBR = (\rho_4 - \rho_7) \div (\rho_4 + \rho_7)$, and ρ_i denotes the surface reflectance of Landsat band i . Although RdNBR was developed for assessing post-fire effects and will not be ideal for assessing burned and unburned pixels (Verstraete and Pinty 1996; Pereira 1999; Smith *et al.*, 2007a; Lentile *et al.* 2009; Heward *et al.*, 2013), its classification schema does include an unburned to low severity classification category and therefore we sought to explore its utility in meeting question (2). The RdNBR images of each fire were produced following the methodology of Miller and Thode (2007), and are accompanied by burned/unburned thresholds, manually identified for each fire using interpretations of the dNBR and RdNBR data, raw pre- and post-fire satellite imagery, plot data (if available) and the analysts' own judgment (Eidenshink *et al.* 2007).

Methods

RdNBR burned area maps

Raster burned area maps were produced from the MTBS RdNBR images, by applying the burned/unburned threshold provided in the MTBS metadata to the whole image subset. An additional set of maps was produced by applying the threshold only inside the MTBS perimeter of the burned areas, in order to verify the potential of using the RdNBR data to refine the existing polygons.

MIRBI and CSI area burned maps

Additional semi-manual area burned maps were derived for the four fires by applying thresholds to spectral indices previously used in similar environments: the MIRBI spectral index (Trigg and Flasse 2001; Smith *et al.* 2007b) and the CSI index (Smith *et al.* 2005). MIRBI was originally formulated for MODIS data, and is a linear combination of MODIS bands 6 (1.628-1.652 μm) and 7 (2.105–2.155 μm); the index was designed to have isolines orthogonal to the spectral changes induced by fire and it was observed to be insensitive to vegetation type (Trigg and Flasse 2001). Smith *et al.* (2007b) tested the broader applicability of this method using Landsat TM/ETM+ imagery and demonstrated that in savannah systems MIRBI, alongside linear spectral unmixing, outperformed other tested approaches. The general formulation of MIRBI for Landsat imagery is: $\text{MIRBI} = 10 \cdot \rho_7 - 9.8 \cdot \rho_5 + 2.0$, where ρ_7 = TM band 7 reflectance (2.08-2.35 μm) and ρ_5 = TM band 5 reflectance (1.55-1.75 μm) (Smith *et al.* 2007b). Given past studies indicated that MIRBI thresholds around 2.0 provided optimal burned/unburned discrimination, our analysis started at this threshold and sequentially evaluated alternative thresholds at 0.05 intervals. An optimal threshold was selected for each study area, by selecting the value that produced the most accurate classification when compared to the reference imagery described in the next section.

The Char Soil Index (CSI), defined as ρ_4/ρ_5 , i.e. the simple ratio of ρ_4 =TM band 4 reflectance (0.76-0.90 μm) and ρ_5 = TM band 5 reflectance (1.55-1.75 μm). CSI was developed by Smith *et al.* (2005) and consequently applied in several studies (Smith *et al.* 2007b; Stroppiana *et al.* 2012) that demonstrated it to be an effective area burned mapping approach in both savanna and Mediterranean ecosystems. Following the MIRBI process, a similar CSI threshold was determined.

For each spectral index approach we additionally constrained the resultant burned / unburned classification by the MTBS perimeter to evaluate the potential of a coupled (MTBS perimeter + index) approach with indices other than the RdNBR.

Reference data

Key to any robust accuracy assessment is the application of representative, independent validation reference data that is inherently more accurate than the product to be evaluated (Smith *et al.* 2002; Boschetti *et al.* 2006). While ground data and aerial surveys can

potentially yield reference data more accurate than high resolution remote sensing data, their potential use for retrospectively validating burned area products is very limited, as the collection of new data is, by definition, impossible.

Consequently, the use of remotely sensed data as reference is in many cases the only viable option: the international Global Burned Area Satellite Validation Protocol, endorsed by the Committee on Earth Observation (CEOS), requires that when satellite data are used as reference data they should: (A) ideally have a higher spatial resolution than the data used to generate the area burned product, (B) exhibit spectral and radiometric resolution adequate for the unambiguous identification of burned from unburned areas, and (C) be acquired before any vegetation recovery, and/or removal of char and ash, i.e. within weeks after the fire event in savannah and grassland ecosystems (Boschetti *et al.* 2009; Picotte and Robertson 2011).

Those conditions can be usually met for the validation of coarser resolution (250m-1km), where Landsat-derived maps are used as reference dataset. However, when Landsat resolution burned area maps are used as the classification dataset, it is problematic to find higher resolution reference data. This is because imagery with very high spatial resolution (i.e. 1-4m) is only sporadically available, and often does not have sufficient spectral resolution to allow for the unambiguous identification of burned areas. For instance, most aerial and satellite very high resolution sensors acquire visible, panchromatic and near-infrared imagery, which provides very poor discrimination between dark soil, dark vegetation and burned areas.

Given the unavailability of higher resolution imagery, visual interpretation of Landsat images has been often used as reference data (Brewer *et al.* 2005; Petropoulos *et al.* 2010; Oliveira *et al.* 2012; Stroppiana *et al.* 2012). Visual interpretation of the Landsat data by a well-trained expert generally yields the most accurate results, and can be assumed to be the best possible classification of the input data, against which the performance of automatic classification algorithms can be compared.

In the current study we created our reference data via visual interpretation of false color composites (Landsat bands 7:4:5, Figure 1 and Bands 7:4:3); the 1-2 m NAIP aerial imagery did not have sufficient spectral resolution to discriminate reliably between burned and unburned areas, but was used as an additional data source to aid the interpreter in the visual

interpretation of the Landsat data. The digitization was conducted by using a minimum mapping unit of 1 Landsat pixel, thus avoiding any simplification of the polygon boundaries. As a result of the visual interpretation, each pixel of the selected study areas (>1 million per fire) was classified as either burned or unburned. Uncertain pixels at the edges of the area burned were alternately classified as burned/unburned. The confusion matrix between the reference data, the rasterized MTBS polygons, and the six maps obtained from the spectral indices (two maps per index, one applied to the whole study area, and one constrained to the MTBS polygons) was used to calculate overall accuracy, omission / commission errors, and total area burned bias.

Results and Discussion

Accuracy of burned area MTBS polygons

Figures 2 and 3 show, for the four fires, the reference perimeters overlaid on a Landsat post-fire false color composite, as well as the MTBS fire polygons, and the raster maps obtained by thresholding the three spectral indices. In each of Figures 2 and 3 the colors indicate agreement and disagreement between the reference data and the classification: commission errors within and outside the fire perimeter are plotted in red and yellow respectively; correctly classified burned and unburned areas are plotted in white and black respectively; omission errors are plotted in green. The accuracy metrics obtained from the confusion matrix are reported in Table 1. The MTBS perimeters had overall accuracies across all four fires ranging from 94.2 to 97.6% (Table 1). However, as evident in Figures 2 and 3, the MTBS perimeters often over-simplify the burned area polygons when the areas are very fragmented, and do not map large unburned islands. This causes a significant bias in area burned: the MTBS perimeters overestimated the area burned on all fires, by a percentage ranging from 4.1% to 16.8%.

Accuracy of spectral index based burned area maps

The burned area map obtained through RdNBR threshold on the whole image had high burned area commission errors (17.2-42.4%), evident in Figures 2 and 3, and consequently large overestimations of area burned (13.8-58.6%). Application of the MIRBI spectral index, with an individual optimal threshold determined for each fire, provided overall accuracies of

area burned ranging from 92.2 to 97.9% (Table 1), with compensation of the omission and commission errors resulting in a slight underestimations of the total area burned (0.1-2.1%). Across all four fires, the MIRBI thresholds produced a burned commission error of 2.1-10.8% (Table 1). The CSI spectral index produced accuracies of area burned ranging from 96.3 to 98.6% (Table 1), with low omission and commission errors (Figures 2a and 3b) and small over/under estimation of area burned (<3%).

The slight difference in performance between the three spectral indices can be explained given the RdNBR threshold, which is provided by the MTBS project, was never intended to be used outside the burn perimeter. In contrast, the CSI and MIRBI index thresholds were developed by optimizing the spectral separation between unburned and burned surfaces in each study site.

Accuracy of spectral index maps constrained by MTBS polygons

Constraining the RdNBR spectral index by the MTBS perimeters consistently improved the accuracy for the four fires (~97% on all fires), and significantly reduced the burned area bias compared not only to the un-constrained RdNBR, but also to the MTBS polygons. The resulting maps had a slight underestimation of the area burned (<3%). This illustrates that the burned/unburned threshold provided as part of the MTBS metadata for each fire should not be used to generate an alternative burned area map, but in a similar manner to Abatzalguo and Kolden (2013) who excluded unburned and low severity from the MTBS perimeters, at a minimum the unburned RdNBR spectral index threshold could be used to further refine the vector MTBS polygons.

When constrained by the MTBS perimeter, MIRBI showed slight increases in accuracy for all fires except the Burnt Fire. As can be expected the constrained maps exhibited lower burned commission errors (0.9-2.5%). However, because of the significant omission error, the total burned area was underestimated (1.4-10.8%, Table 1). Constraining the CSI map by the MTBS polygons provided the highest accuracy of the three spectral indices. Overall, the CSI spectral index was the most consistent when producing accurate area burned maps.

Conclusions

To recap, the specific questions we sought to address for the MTBS area burned product were:

- (1) What is the areal accuracy of the burned area MTBS polygons?
- (2) Can the accuracy be improved by applying a simple threshold to spectral indices within the polygons?

In terms of (1), validation over four large fire events in a shrub-steppe environment showed that, despite having high classification accuracies, the MTBS perimeters systematically overestimated the area burned, between 4 and 16.8% in the four validation sites. These findings suggest that caution is needed when area estimates, derived from the MTBS burned area perimeters, are used directly for scientific investigations (e.g., to evaluate burned area trends within temporal series). In terms of (2), this study shows that for shrub-steppe environments the area burned estimates can be significantly improved if a simple threshold on spectral index values is used within the MTBS perimeters. The CSI and MIRBI indices provided the highest accuracy (>90%), but require the estimation of a different optimal threshold for each fire and thus are not ideal within an automated system. The use of RdNBR with the burned/unburned threshold provided by the MTBS metadata produced results that, albeit variable in accuracy across the four cases, are very close to the results obtained with the other two indices. A simple but effective route to improve the MTBS burned area product would be to apply a spectral index designed to discriminate burned and unburned surfaces to the pixels within the MTBS burned area polygon. The spectral indices should be selected on a fire-regime specific basis from the available burned area mapping literature (i.e. not severity indices) and ideally if automation is desired, these indices should not require determination of case-specific optimal thresholds. This case study clearly demonstrates the need to extend MTBS validation assessments to other fire regimes and to evaluate the potential of other burned area mapping spectral indices to improve the polygon estimates.

Acknowledgments

This work was partially funded by the National Aeronautics and Space Administration (NASA) under awards NNX11AO24G and NNX11AF19G.

References

- Abatzagluo JT, Kolden CA (2011) Climate change in western US deserts: Potential for increased wildfire and invasive annual grasses, *Rangeland Ecology and Management* 64, 5, 471-478.
- Abatzagluo JT, Kolden CA (2013) Relationships between climate and macroscale area burned in the western United States, *International Journal of Wildland Fire* 22, 7, 1003-1020.
- Baker WL (2006) Fire and restoration of sagebrush ecosystems, *Wildlife Society Bulletin* 34, 1, 177-185.
- Boschetti L, Brivio PA, Eva HD, Gallego J, Baraldi A, Gregoire J-M (2006) A sampling method for the retrospective validation of global burned area products, *IEEE Transactions on Geoscience and Remote Sensing* 44, 7, 1765-1772.
- Boschetti L, Roy DP, Justice CO (2009) International Global Burned Area Satellite Product Validation Protocol Part I – production and standardization of validation reference data (to be followed by part II – accuracy reporting). Available online: <http://lpvs.gsfc.nasa.gov/PDF/BurnedAreaValidationProtocol.pdf>
- Brewer CK, Winne JC, Redmond RL, Opitz DW, Mangrich MV (2005) Classifying and mapping wildfire severity: a comparison of methods, *Photogrammetric Engineering and Remote Sensing* 71, 11, 1311-1320.
- Chambers JC, Roundy BA, Blank RR, Meyer SE, Whittaker A (2007) What makes Great Basin sagebrush ecosystems invasible by *Bromus tectorum*? *Ecological Monographs* 77, 1, 117-145.
- Crawford JA, Olson RA, West NE, Mosley JC, Schroeder MA, Whitson TD, Miller RF, Gregg MA, Boyd CS (2004) Synthesis paper – Ecology and management of sage-grouse and sage-grouse habitat, *Journal of Range Management* 57, 1, 2-19.
- Dillon GK, Holden ZA, Morgan P, Crimmins MA, Heyerdahl EK, Luce CH (2011) Both topography and climate affected forest and woodland burn severity in two regions of the western US, 1984 to 2006, *Ecosphere* 2, 12, Article 130.
- Eidenshink J, Schwind B, Brewer K, Zhu Z, Quayle B, Howard S (2007) A project for monitoring trends in burn severity, *Journal of Fire Ecology* 3, 3-21.
- Heward H, Smith AMS, Roy DP, Tinkham WT, Hoffman CM, Morgan P, Lannom KO (2013) Is burn severity related to fire intensity? Observations from landscape scale remote sensing, *International Journal of Wildland Fire* 9, 910-918. doi: 10.1071/WF12087.

- Kolden CA, Lutz JA, Key CH, Kane JT, van Wagtenonk JW (2012) Mapped versus actual burned area within wildfire perimeters: Characterizing the unburned, *Forest Ecology and Management* 286, 38-47.
- Lannom KO, Tinkham WT, Smith AMS, Abarzoglou J, Newingham BA, Hall T, Morgan P, Strand EK, Paveglio Y, Anderson JW, Sparks AM (2014) Defining extreme wildland fires using geospatial and ancillary metrics, *International Journal of Wildland Fire*, doi: 10.1071/WF13065.
- Lentile LB, Holden ZA, Smith AMS, Falkowski MJ, Hudak AT, Morgan P, Lewis SA, Gessler PE, Benson NC (2006) Remote sensing techniques to assess active fire characteristics and post-fire effects, *International Journal of Wildland Fire* 15, 3, 319-345, doi: 10.1071/WF05097.
- Lentile LB, Smith AMS, Hudak AT, Morgan P, Bobbitt M, Lewis SA, Robichaud P (2009) Remote sensing for prediction of 1-year post-fire ecosystem condition, *International Journal of Wildland Fire* 18, 594-608.
- Lund GH (2007) Accounting for the world's rangelands, *Rangelands* 2, 3-10.
- Masek JG, Huang CQ, Wolfe R, Cohen W, Hall F, Kutler J, Nelson P (2008) North American forest disturbance mapped from a decadal Landsat record, *Remote Sensing of Environment* 112, 6, 2914-2923, doi: 10.1016/j.rse.2008.02.010.
- Masek JG, Vermote EF, Saleous NE, Wolfe R, Hall FG, Huemmrich KF, Gao F, Kutler J, Lim TK (2006) A Landsat surface reflectance dataset for North America, 1990-2000, *IEEE Geoscience and Remote Sensing Letters* 3, 1, 68-72, doi: 10.1109/LGRS.2005.857030.
- Miller JD, Thode AE (2007) Quantifying burn severity in a heterogeneous landscape with a relative version of the delta Normalized Burn Ratio (dNBR), *Remote Sensing of Environment* 109, 66-80.
- Morton DC, Collatz GJ, Wang D, Randerson JT, Giglio L, Chen Y (2012) Satellite-based assessment of climate controls on US burned area, *Biogeosciences* 9, 7853-7892, doi: 10.5194/bgd-9-7853-2012.
- Oliveira SLJ, Pereira JMC, Carreiras JMB (2012) Fire frequency analysis in Portugal (1975-2005), using Landsat-based burnt area maps, *International Journal of Wildland Fire* 21, 48-60. doi.org/10.1071/WF10131.
- Pereira JMC, Sá ACL, Sousa AMO, Silva JMN, Santos TN, Carreiras JMB (1999) Spectral characterisation and discrimination of burnt areas. In *Remote Sensing of Large Wildfires in the European Mediterranean Basin*, pp.123-138 (E. Chuvieco, ed), Springer-Verlag, Berlin.

- Petropoulos GP, Vadrevu KP, Xanthopoulos G, Karantounias G, Scholza M (2010) A comparison of spectral angle mapper and artificial neural network classifiers combined with Landsat TM imagery analysis for obtaining burnt area mapping, *Sensors* 10, 1967-1985, doi: 10.3390/s100301967.
- Picotte JJ, Robertson K (2011) Timing constraints on remote sensing of wildland fire burned area in the southeastern US, *Remote Sensing* 3, 8, 1680-1690, doi: 10.3390/rs3081680.
- Randerson, JT, Chen, Y, Werf, GR, Rogers, BM, & Morton, DC (2012). Global burned area and biomass burning emissions from small fires. *Journal of Geophysical Research: Biogeosciences* (2005–2012), 117(G4).
- Riley KL, Abatzoglou JT, Greenfell IC, Klene AE, Heinsch FA (2013) The relationship of large fire occurrence with drought and fire danger indices in the western USA, 1984-2008: the role of temporal scale, *International Journal of Wildland Fire* 22, 894-909.
- Roy DP, Boschetti L, Justice CO, Ju J (2008) The collection 5 MODIS burned area product – Global evaluation by comparison with the MODIS active fire product, *Remote Sensing of Environment* 112, 3690-3707, doi: 10.1016/j.rse.2008.05.013.
- Smith AMS, Wooster MJ, Drake NA, Dipotso FM, Perry GLW (2005) Fire in Africa savanna: testing the impact of incomplete combustion on pyrogenic emission estimates, *Ecological Applications* 15, 3, 1074-1082.
- Smith AMS, Wooster MJ, Powell AK, Usher D (2002). Texture based feature extraction: application to burn scar detection in Earth Observation Imagery, *International Journal of Remote Sensing* 23, 1733-1739.
- Smith AMS, Lentile LB, Hudak AT, Morgan P (2007a) Evaluation of linear spectral unmixing and dNBR for predicting post-fire recovery in a N. American ponderosa pine forest, *International Journal of Remote Sensing* 22, 20, 5159-5166.
- Smith AMS, Drake NA, Wooster MJ, Hudak AT, Holden ZA, Gibbons CJ (2007b) Production of Landsat ETM+ Reference Imagery of Burned Areas within Southern African Savannas: Comparison of Methods and Application to MODIS, *International Journal of Remote Sensing* 28, 12, 2753-2775, doi: 10.1080/01431160600954704.
- Stringham TK, Kruger WC, Shaver PL (2003) State and transition modeling: An ecological process approach, *Journal of Range Management* 56, 2, 106-113, doi: 10.2307/4003893.
- Stroppiana D, Bordogna G, Carrara P, Boschetti M, Boschetti M, Brivio PA (2012) A method for extracting burned areas from Landsat TM/ETM plus images by soft aggregation of multiple Spectral Indices and a region growing algorithm, *ISPRS Journal of Photogrammetry and Remote Sensing* 69, 88-102, doi: 10.1016/j.isprsjprs.2012.03.001.

- Sunderman SO, Weisberg PJ (2011) Remote sensing approaches for reconstructing fire perimeters and burn severity mosaics in desert spring ecosystems, *Remote Sensing of Environment* 115, 2384-2389, doi: 10.1016/j.rse.2011.05.001.
- Trigg S, Flasse S (2001) An evaluation of different bi-spectral space for discriminating burner shrub-savannah, *International Journal of Remote Sensing* 22, 13, 2641-2647, doi: 10.1080/01431160110053185.
- Verstraete MM, Pinty BP (1996) Designing optimal spectral indexes for remote sensing applications. *IEEE Transactions on Geosciences and Remote Sensing* 34, 5, 1254-1265.
- West NE, Young JA (2000) Intermountain valleys and lower mountain slopes. In 'North American terrestrial vegetation, Second edition', Eds Barbour MG, Billings WD, pp. 255-284, Cambridge University Press, Cambridge, United Kingdom.
- Zheng, D, Heath, LS, Ducey, MJ, & Smith, JE (2011). Carbon changes in conterminous US forests associated with growth and major disturbances: 1992–2001. *Environmental Research Letters*, 6(1), 014012.

Table 1. Burned area accuracy assessment of the optimal CSI, MIRBI and RdNBR thresholds, MTBS perimeters, and CSI, MIRBI and RdNBR thresholds constrained by MTBS perimeters for the four fires. All accuracies are expressed as percent.

Fires	MTBS perimeters	Maps from Index Threshold			Maps from Index Threshold constrained to MTBS perimeters		
		CSI	MIRBI	RdNBR	CSI(P)	MIRBI(P)	RdNBR(P)
Burnt -	Index Threshold	0.81	1.95	135	0.81	1.95	135
	Overall Accuracy	98.0	97.3	70.7	98.1	97.6	96.7
	Commission Burned	2.6	6.6	42.4	1.5	2.5	6.4
	Commission Unburned	1.7	1.1	1.6	2.3	2.3	1.1
	Omission Burned	4.1	2.8	1.3	3.4	3.4	1.6
	Omission Unburned	1.0	2.6	47.5	1.0	1.7	4.4
Total Area Burned (bias, %)	-0.02	-1.2	58.6	-2.6	-1.0	-0.4	
Dry Creek -	Index Threshold	0.73	0.4	70.0	0.73	0.4	70.0
	Overall Accuracy	96.3	92.2	91.5	97.4	95.1	96.6
	Commission Burned	4.4	10.8	17.9	1.2	2.2	3.8
	Commission Unburned	3.4	6.4	2.1	3.2	6.0	3.2
	Omission Burned	6.8	12.7	3.6	6.6	12.5	6.4
	Omission Unburned	2.2	5.3	11.0	0.6	1.0	1.8
Total Area Burned (bias, %)	-2.5	-2.2	13.8	-5.7	-10.8	-3.0	
Hogups -	Index Threshold	0.73	2.0	150	0.73	2.0	150
	Overall Accuracy	97.2	95.8	90.5	97.8	97.2	97.1
	Commission Burned	3.8	7.4	22.8	2.0	1.7	4.7
	Commission Unburned	2.3	2.9	2.7	2.3	3.3	2.1
	Omission Burned	5.2	7.5	6.3	4.7	7.6	4.8
	Omission Unburned	1.7	2.9	10.7	1.0	0.7	2.1
Total Area Burned (bias, %)	-1.4	-1.1	17.8	-3.7	-6.1	-0.3	
Scorpio -	Index Threshold	0.81	1.9	150	0.81	1.9	150
	Overall Accuracy	98.6	97.9	88.8	99.1	98.4	97.4
	Commission Burned	1.5	2.1	17.2	0.7	0.9	3.0
	Commission Unburned	1.3	2.2	2.4	1.2	2.3	2.2
	Omission Burned	1.3	2.2	2.0	1.2	2.3	2.2
	Omission Unburned	1.6	2.1	20.7	0.7	0.9	3.0
Total Area Burned (bias, %)	0.2	-0.1	18.4	-1.3	-1.4	0.8	

CSI – char soil index, MIRBI – mid infrared bi-spectral index, RdNBR – relativized differenced normalized burn ratio, (P) denotes perimeter

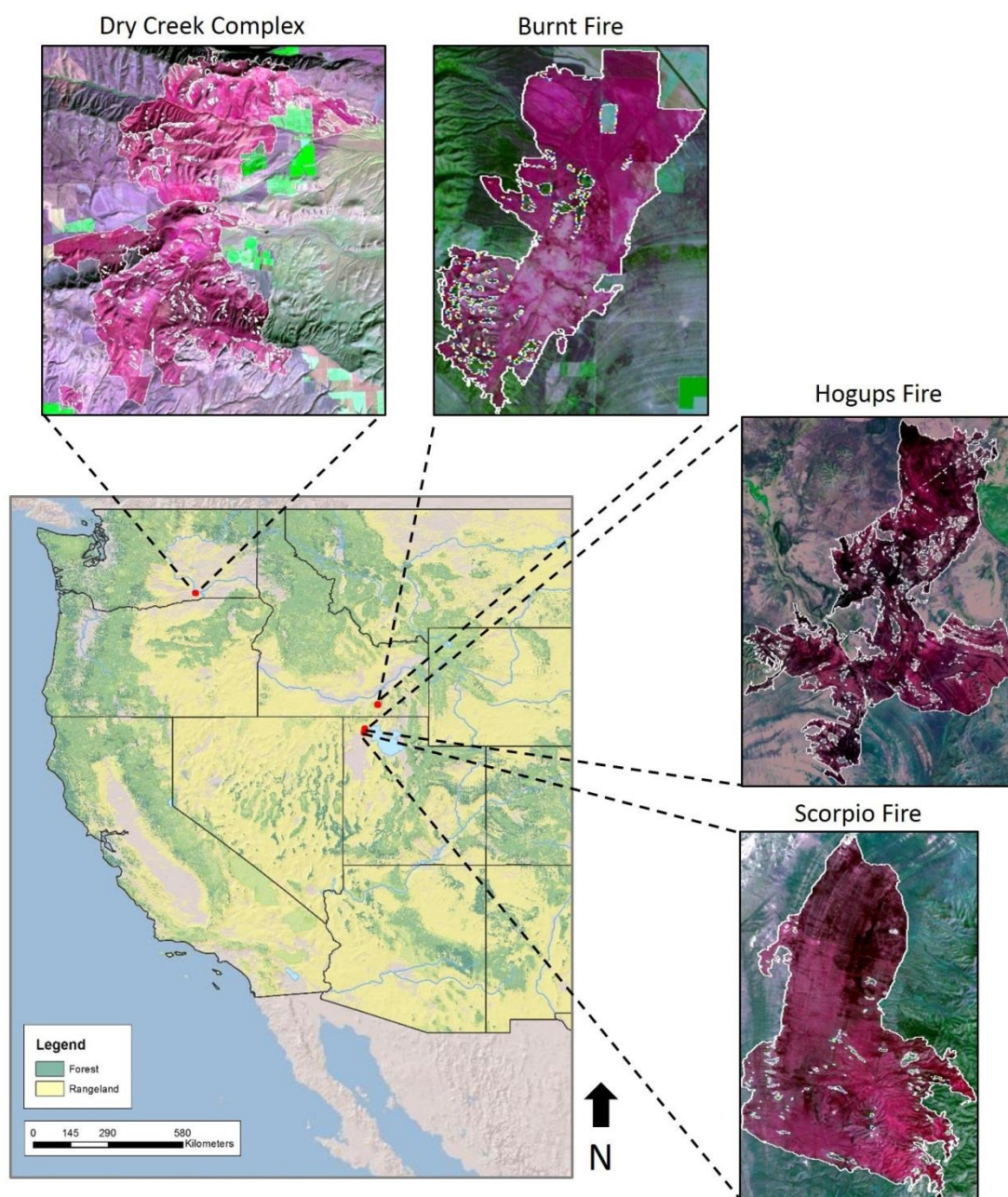


Figure 1. Map of western United States forested and rangeland extent, which include shrub steppe, and the location of the investigated fires (Burnt, Dry Creek Complex, Hogups, and Scorpio). The Burnt fire burned 3,499 ha in south-central Idaho in early July, the Dry Creek Complex burned 18,592 ha in south-central Washington, the Hogups fire burned 10,425 ha in northwest Utah in early August, and the Scorpio fire burned 5,789 ha in northwest Utah in late June.

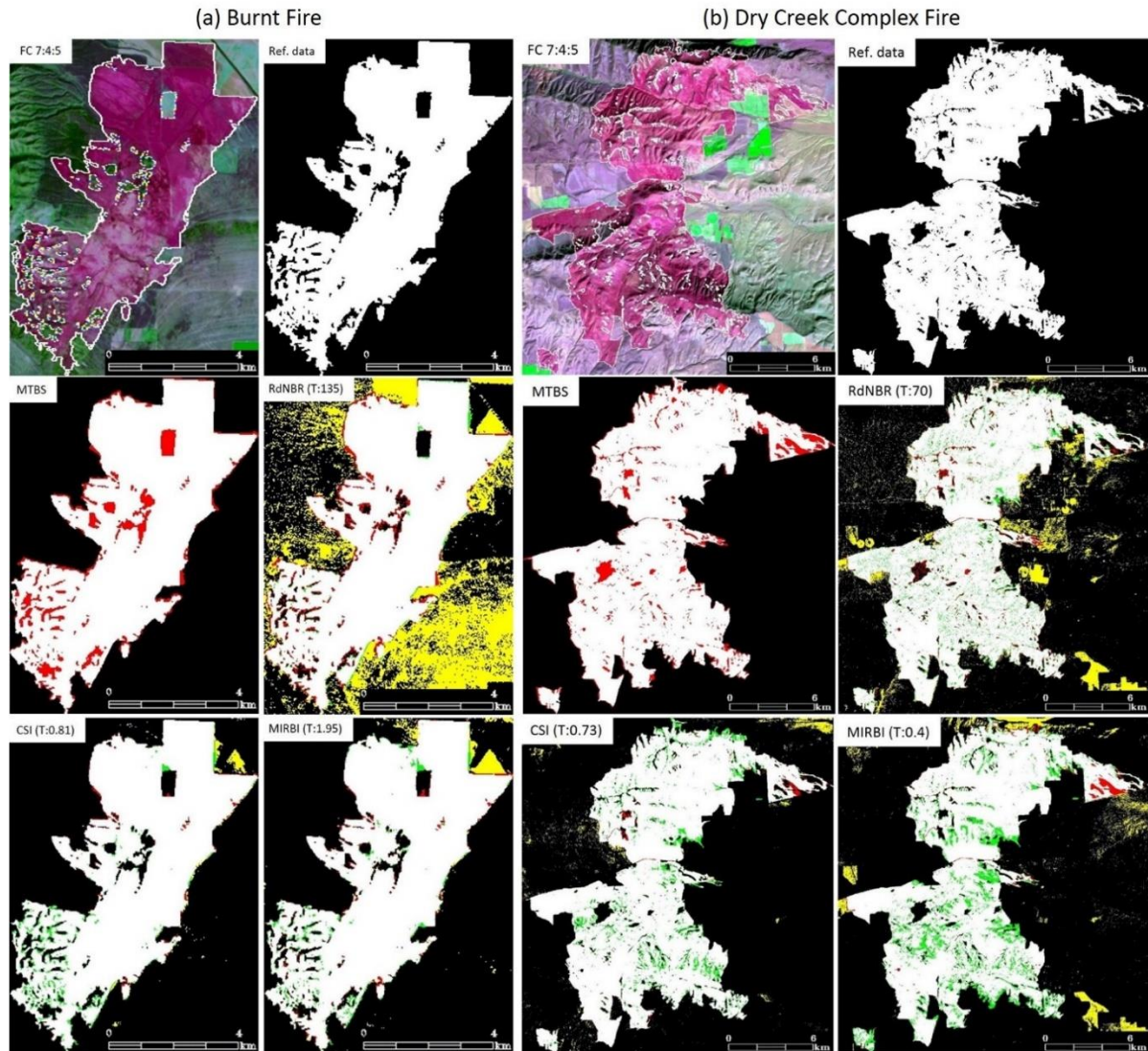


Figure 2. Remote sensing imagery for the (a) Burnt fire and (b) Dry Creek Complex fire showing a Landsat TM false color composite (R:band 7, G: band 4, B:band 5), the visually interpreted reference data, MTBS-perimeter with commission errors shown in red, and RdNBR, CSI, and MIRBI burned area maps displaying correctly classified burned area (white) and non-burned area (black), commission (red) and omission errors (green) inside the burn perimeter, and commission errors (yellow) outside the burn perimeter. Threshold values used for the classification are reported for each index.

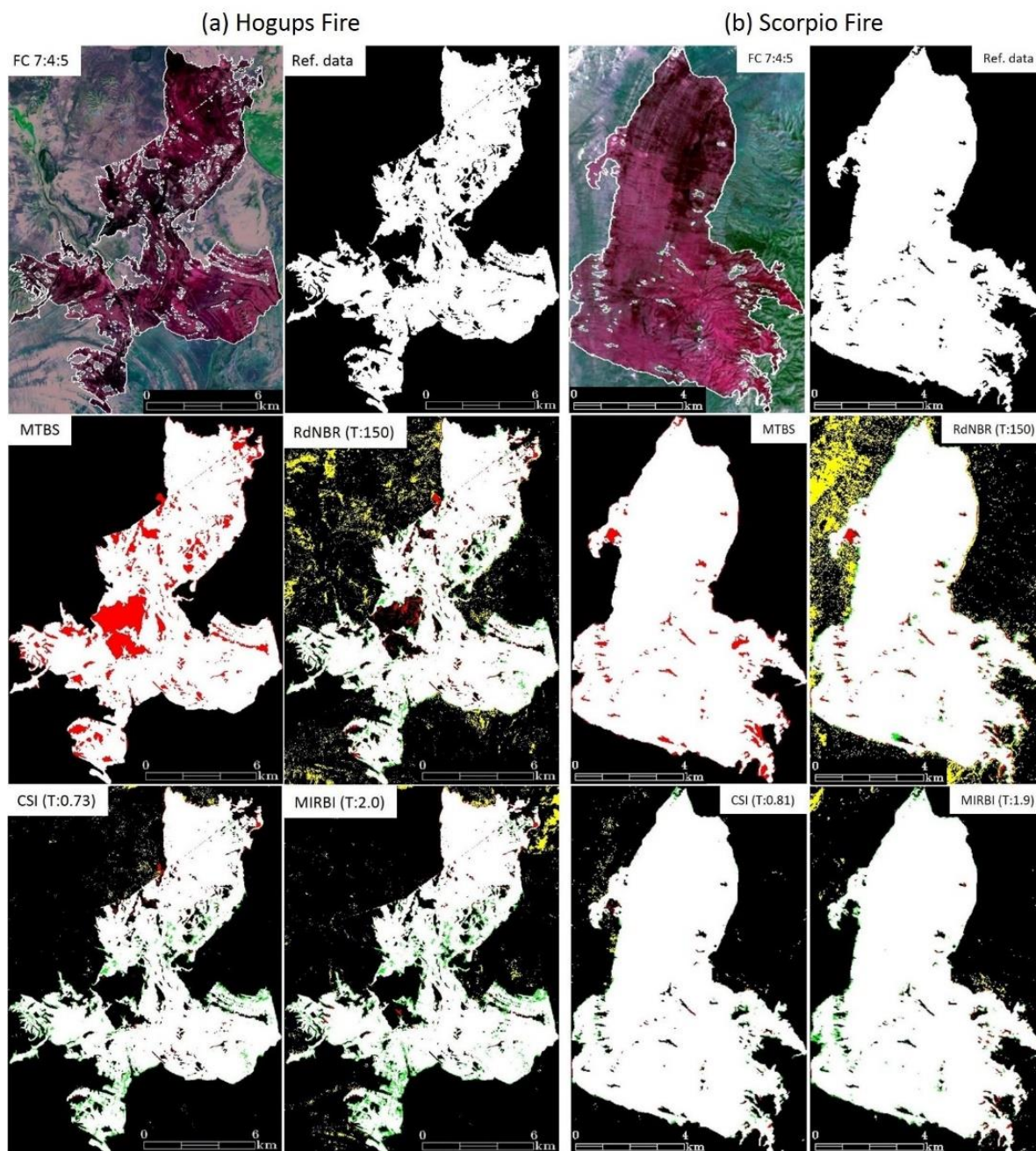


Figure 3. Remote sensing imagery for the (a) Hogups fire and (b) Scorpio fire showing a 7:4:5 band false color composite, the manually-derived burn area map, MTBS-perimeter with commission errors overlaid, and RdNBR, CSI, and MIRBI burned area maps displaying correctly classified burned area (white) and non-burned area (black), commission (red) and omission errors (green) inside the burn perimeter, and commission errors (yellow) outside the burn perimeter. Threshold levels are inset for each of the indexes.

Chapter 3

Evaluating the Dependence of Sagebrush Trace Gas Emission Factors on Seasonal Phenology

Abstract

Air quality impacts from biomass burning are of considerable concern in most fire prone ecosystems. Although fire is a common disturbance agent in shrub-steppe, few studies have specifically evaluated emission factors in these semi-arid to arid environments. Given complimentary observations in southern Africa, a compelling question that arises is whether the seasonality of sagebrush phenology influences emission factors. In this preliminary study we collected, dried, and burned Wyoming big sagebrush (*Artemisia tridentata* Nutt. ssp. *wyomingensis* Beetle and Young) throughout the burn season (May-October) to help isolate seasonal influences, such as sagebrush phenology, on emission factors (EF) of common carbonaceous (CO, CO₂) and nitrogenous (NO, NO₂, NO_x) trace gas species. Results suggest a strong seasonal dependence of EF_{CO₂} (n=8 {10 replicates}, $p < 0.001$) with a weaker accompanying EF_{CO} trend (n=11 {10 replicates}, $p = 0.065$). No significant trend in nitrogenous trace gas emission factors was observed (n=11 {10 replicates}, $p = 0.076$). Modified combustion efficiency (MCE) increases throughout the season suggesting that phenological changes are an important determinant of the ratio of complete and incomplete combustion products.

Introduction

Sagebrush (*Artemisia* spp.) ecosystems occupy >500,000 km² in the western U.S., covering most of the Great Basin as well as large areas in Wyoming and southern Idaho (Miller et al., 2011) (Figure 1). Fire is an important disturbance agent in these ecosystems, altering nutrient availability and wildlife habitat (Chambers et al. 2007; Crawford et al. 2004). In addition to wildfires, prescribed fire is a common practice in sagebrush ecosystems; its uses ranging from improving browse for wildlife and livestock (Beck et al. 2009, 2012; Clark et al., 2014; Davis et al., 2007) to controlling invasive species (Davies et al. 2007, 2012; DiTomaso et al. 2006) and reducing fuel load (Davies et al., 2012). A large portion of fire research and management has focused on the effects of prescribed fire on

Greater Sage-Grouse (*Centrocercus urophasianus*) and ungulate species through manipulation of cover and browse (Beck et al. 2009; Nelle et al., 2000; Pyle and Crawford, 1996; Rhodes et al., 2010). Recently, interest has shifted toward the use of prescribed fire for controlling invasive species such as cheatgrass (*Bromus tectorum* L.) and medusahead (*Taeniatherum caput-medusae* L. Nevski) (Davies et al. 2007, 2012; DiTomaso et al. 2006).

Regardless of the prescribed fire objective, an overarching concern for land managers implementing prescribed fires near the wildland urban interface (WUI) is air quality. Burn permits are closely monitored/regulated due to the adverse health effects caused by smoke emissions, especially particulate matter (PM_{2.5}) and photochemical smog. These effects are often exacerbated near urban areas where there is a higher density of people sensitive to poor air quality. PM_{2.5} is an air quality concern because it can accumulate in the lungs and has been linked with increased risk of heart disease (Hardy et al., 2001). Particulate matter is primarily produced via incomplete combustion processes and is strongly negatively correlated to modified combustion efficiency (MCE) (Yokelson et al., 2013). MCE is calculated using excess mixing ratios (mixing ratios exceeding background mixing ratios, designated by ΔX) following the calculation presented in Ward and Radke (1993):

$$\text{Modified Combustion Efficiency (MCE)} = \frac{\Delta C_{CO_2}}{\Delta C_{CO_2} + \Delta C_{CO}}$$

where ΔC_{CO_2} = excess carbon mixing ratio emitted as CO₂ and ΔC_{CO} = excess carbon mixing ratio emitted as CO. As MCE declines, more particulate matter is produced and emitted in smoke. MCE has also been observed to be seasonally dependent (Hoffa et al., 1999; Korontzi et al., 2003). In African savannas, lower MCE in the early dry season resulted in higher emissions of smoldering combustion products, such as CO, CH₄, and NMHC (non-methane hydrocarbons), whereas higher MCE in the mid-to-late dry season resulted in higher emissions of flaming combustion products, such as CO₂ (Justice et al., 2002; Korontzi et al., 2003; Yokelson et al., 2011).

Like PM_{2.5}, NO_x (NO and NO₂) emitted from fires is an additional local and regional air quality concern (Jaffe et al., 2004) as, via photolysis, it is the primary precursor for tropospheric ozone (O₃), a key ingredient of photochemical smog (Khalil and Rasmussen, 1988; Seinfeld and Pandis, 1998). O₃ production is likely enhanced within semi-arid to arid

environments where warm temperatures and infrequent cloud cover are common during the typical fire season.

Similar to major carbonaceous species, NO_x emissions have also been observed to be seasonally dependent. Across multiple ecosystems, NO_x emissions have been found to decrease 20-40% from early season fires to late season fires (Lapina et al., 2008; Mebust and Cohen, 2013). NO_x emissions are typically produced via flaming combustion and thus the increase in smoldering combustion found in late season fires may be correlated with the decrease in NO_x emissions (Lapina et al., 2008). Battye and Battye (2002) and Yokelson et al. (2011), however, found a very poor correlation ($R^2 = 0.11$) between MCE and NO_x emission factors, indicating the influence of other factors such as fuel nitrogen content. Little research has been undertaken to uncover the role of fuel nitrogen in NO_x emissions (Lacaux et al., 1996; Burling et al., 2010). Seasonal influences are important because management fires in shrub-steppe typically occur in early spring (April) or late fall (November) to minimize risk of escape (Davies et al. 2013). To date, few studies have specifically looked at trace gas emissions from sagebrush fires at any point in the typical fire season.

In addition to moisture content, sagebrush phenology represents a large potential driver of trace gas emission factors. Wyoming big sagebrush phenology has been briefly documented in the literature (DePuit and Caldwell, 1973; Fernandez and Caldwell, 1975; Kelsey et al., 1982, Wilt and Miller, 1992). Generally, big sagebrush emerges from dormancy in early May, experiences maximum growth in late May to early June, and starts to enter dormancy around mid-November (DePuit and Caldwell, 1973). During the summer months, big sagebrush accumulates terpenes and terpenoids, compounds thought to possess phytotoxic, cytotoxic, antimicrobial, and browse deterrent properties (Kelsey et al., 1982). There is also a decline in non-structural carbohydrates and protein over this time period (Kelsey et al., 1982). It is largely unknown how this phenological cycle effects trace gas emissions from sagebrush fires. Therefore, the main objective of this study was to see if carbonaceous and nitrogenous trace gas species emitted from sagebrush fires were seasonally dependent. The specific questions we sought to address in this study are:

- (1) Does timing of sagebrush fires influence emission factors of common carbonaceous (CO, CO₂) and nitrogenous (NO, NO₂, NO_x) trace gas species?

- (2) How do phenology changes in sagebrush influence the observed modified combustion efficiency within these fires?

Methods

Experimental setup

Fire experiments were conducted at the Idaho Fire Institute of Research and Education (IFIRE), located in a climatically controlled environment that is shielded from weather effects. The facility consists of two adjoining rooms, each roughly 6 m x 8 m x 6 m high. In the combustion room, a 0.5 m x 0.6 m exhaust stack with a 1 m x 1.5 m opening extends from 2 m above the burn table and exits the side of the building. Smoke sampling ports are located on each side of the square exhaust stack, 1 m before the stack exits the building. Smoke is drawn through 0.635 cm diameter Teflon tubing from the sampling ports to gas analyzers (distance of <5 m) in the adjacent control room.

Fuel descriptions and laboratory setup

All fuel burned in this study was collected at the Columbia National Wildlife Refuge, WA, located at 46.965°N -119.251°W (Figure 1). The collection site had uniform topography (elevation range: 290-300m) and a fairly uniform species distribution of big sagebrush, bluebunch wheatgrass, and cheatgrass. At the field site, 5 samples (~200 g each) of big sagebrush were collected, split into two separate samples, and weighed *in situ* using a Sartorius Praxum 5101 scale (accurate to 0.1 g). Samples were collected at randomized points along a grid of transects running perpendicular to the site slope. At each collection point, a 0.5 m² quadrat frame was positioned with its upper left corner over the transect point. Sagebrush areal foliage and twig (diameter <0.635 cm) samples were clipped from a vertical projection of the 0.5 m² quadrat frame. After being clipped and weighed, samples were immediately put in coolers and transported back to the IFIRE facility.

All samples were burned on top of a Sartorius EB Series scale (65 kg capacity, accurate to 1 g), to record fuel mass loss throughout the burn period. Big sagebrush samples were constructed in loose burn beds with fuel loads comparable to those in the field, ~0.4 kg m⁻². A small subsample (1-2 grams) of pre-burn live fuel and post-burn ash were also collected and carbon and nitrogen content were analyzed by the Washington State University, Stable

Isotope Core Laboratory. For each ignition, a small amount of 100-proof ethanol was added to the edge of the fuel bed and ignited to provide a uniformly spreading flaming front. Emissions data representing ignition was omitted from the data recorded. Initially, we attempted to burn the sagebrush samples at field moisture content, however, our ignition methods were unsuccessful at all sampling points throughout the season. Consequently, all of the samples were dried in a drying oven for at least 24 hours at 90°C. While this fuel moisture does not exist in the field, we decided to burn dried sagebrush as a test for other seasonal influences (e.g. phenological/physiological influences) on emissions. Moisture content (MC) of the samples was calculated via the oven-dry method:

$$MC = \frac{(wet\ mass - dry\ mass)}{dry\ mass}$$

where wet mass = mass of sample measured immediately after field collection and dry mass = mass of sample measured immediately after being dried in a drying oven for >24 hours at 90°C. Moisture content and fuel consumption measurements are detailed in Table 1.

All of the smoke samples were pumped to the IFIRE facility control room through 0.635 cm diameter Teflon tubing except CO measurements, which were sampled directly at the sampling ports. CO concentrations were measured with a LASCAR carbon monoxide data logger (EL-USB-CO300, Lascar Electronics, Wiltshire, UK) every 10 s. CO₂ and H₂O measurements were made with a LICOR (LI-840A, LI-COR, Lincoln, Nebraska) CO₂/H₂O analyzer every 1 s. The CO₂/H₂O analyzer was not available until early July, and thus no CO₂/H₂O data points were collected from May 22 to July 1. Concentrations of NO and NO₂ were measured with a NO_x analyzer (42i-TL NO_x analyzer, Thermo Fisher Scientific, Waltham, Massachusetts) every 1 min. Smoke velocity and temperature were measured every 1 s with a hot wire anemometer (Model 407123, Extech Instruments, Nashua, New Hampshire) at the location of the sampling ports in the exhaust stack.

Emission factor calculations

Background trace gas mixing ratios in this paper are defined as the average mixing ratio of species_(x) during the 20-30 minutes before each individual burn. Typical CO₂ background mixing ratios ranged from 385-400 ppm; CO background mixing ratios ranged from 0-0.5 ppm; NO_x background mixing ratios ranged from: 1-3 ppb). Excess mixing ratios are those

exceeding the background mixing ratio. Emission factors are commonly calculated using the carbon mass balance method [Ward and Radke, 1993; Yokelson et al., 1999]. The carbon mass balance method provides a good estimate of emissions, however, it assumes that all combusted carbon is volatilized, carbon content of the fuel is known, and the smoke is adequately mixed. Since we were missing measurements of several major carbon species, we were unable to use the carbon mass balance technique to calculate emission factors. Instead, we calculated emission factors using the assumption that trace gases emitted during the burns represented ideal gases. We converted excess mixing ratios (ppmv) to concentrations (g m^{-3}) using the following calculation (Seinfeld and Pandis, 1998):

$$\text{Concentration (g m}^{-3}\text{) of species}_{(x)} = \frac{(MM \times P \times c_{(x)})}{(R \times T)}$$

where MM = molecular mass of species_(x) (g mol^{-1}), P = atmospheric pressure corrected for elevation (mb), $c_{(x)}$ = mixing ratio (mol mol^{-1}), R = gas constant ($0.083145 \text{ m}^3 \text{ mb mol}^{-1} \text{ K}^{-1}$), and T = temperature (K). To find the total mass (g) of species_(x) emitted for each concentration measurement we multiplied the calculated concentration (g m^{-3}) by the volume flux (m^3) emitted through the stack. Volume flux is defined as the volume, 'V', of air emitted over time, 't'. Volume flux was calculated for each concentration measurement with the following equation:

$$\text{Volume flux} = A \times v \times t$$

where A = cross-sectional area of exhaust stack, v = average velocity of air moving through stack, and t = duration of measurement in seconds. Average velocity was determined by dividing the cross-sectional area of the exhaust stack into 12 equal-area grid cells in addition to a 2 cm buffer near the stack walls where air is slowed due to friction and maintains a consistent velocity. A minimum of 30 velocity measurements were taken at the center of each grid cell and at two points along each exhaust stack wall. These velocity measurements were combined in an area-weighted average to find the average velocity of air moving through the exhaust stack. Total mass of gas species_(x) was divided by vegetation dry mass combusted to obtain emission factors in g kg^{-1} . Emission factors in this paper are presented as fire averaged emission factors (average of calculated emission factors over the duration of each fire).

Trends and Sources of Uncertainty

One-way analysis of variance (ANOVA) with Tukey post hoc analysis was used to test for differences across the season for each trace gas species. Examination of the linear regression trendline slope for each emission dataset was used to indicate a significant seasonal trend. All statistical analysis was conducted with R v.3.0.2. We acknowledge the fact that this dataset may be too small to determine a significant trend.

There are several possible sources of uncertainty in regard to the methods used in this study. First, we assumed that all of the measured trace gases produced during combustion exited through the exhaust stack. Similarly, we assumed the velocity of smoke exiting through the exhaust stack was constant over the 1 second sampling time. We also assumed there were negligible losses of measured trace gases due to tube wall loss, condensation, or desorption from the analyzer filters and that pressure (P) in our emission factor calculation was close to local adjusted atmospheric pressure. Additionally, the sensitivity and temporal resolution of our CO sensor is not ideal for emissions analysis.

Results and Discussion

Carbon content of the sagebrush samples generally increased throughout the season (Figure 2b). This increase can be attributed to several phenological events and physiological processes of big sagebrush: 1) as big sagebrush starts to senesce (early July to mid-August) the larger spring leaves and smaller ephemeral leaves are shed (DePuit et al. 1973; Kelsey et al., 1982) resulting in a higher wood-to-foilage ratio in the samples burned, 2) there is a decrease in total non-structural carbohydrates and protein (lower C content) and an increase in terpenoids, fats, and phenolics (higher C content) through the summer months (Kelsey et al., 1982; Wilt and Miller, 1992), and 3) differentiation into woody tissue increases through the summer months (Kelsey et al., 1982). Fuel consumption and nitrogen content were fairly consistent throughout the study at ~86.6% and ~1.7%, respectively (Table 1).

We could not get big sagebrush samples at field moisture content to carry fire throughout the duration of the study, which possibly indicates the importance of other factors including: dry litter and grasses surrounding sagebrush in the field as well as wind and other climatic influences. Generally, higher moisture content of fuels in the early part of the burning

season contributes to the production of greater smoldering combustion emissions such as CO and CH₄ (Hoffa et al. 1999; Korontzi et al. 2003) whereas lower moisture content in the late season contributes to the production of flaming combustion emissions like CO₂ (Yokelson, et al., 2003; Sinha et al., 2003; Akagi et al., 2011). Big sagebrush exhibited a rapid decline in moisture content from 145% in mid-May to 90% in early June and a more gradual decline from 90% in June to 40% in early September (Figure 1). This seasonal trend is consistent with other studies reporting big sagebrush seasonal moisture content (Fischer et al., 1996; Van Epps et al., 1982; Evans et al., 1992).

Despite the fact that the big sagebrush samples were dried, emission factors of CO₂ displayed a notable trend through the fire season, increasing from ~1245 g kg⁻¹ in early July to ~1484 g kg⁻¹ in late October (n=8, 10 replicates, $p < 0.001$) (Figure 2c). A one-way ANOVA, with Tukey post hoc test, between the start date and end date confirmed that these two dates were significantly different ($p < 0.001$). A weaker seasonal trend occurred in EF_{CO}, where EF_{CO} decreased from ~85 g kg⁻¹ mid-May to ~78 g kg⁻¹ in late October (n=11, 10 replicates, $p = 0.065$). The start and end date were not significantly different ($p = 0.99$). Like EF_{CO}, EF_{NO_x} displayed a weak seasonal trend (n=11, 10 replicates, $p = 0.076$) and the start and end sample dates were significantly different ($p < 0.001$). Nitrogen budget analysis indicates we are missing most (>70%) of the original fuel nitrogen, not included in NO_x or in residual ash (Figure 2f). Other studies suggest a large portion of fuel nitrogen may be accounted for as N₂ emissions (Kuhlbusch et al., 1991) or in smaller amounts as smoldering compounds such as NH₃ (Burling et al., 2010).

There is a significant relationship between EF_{CO₂} derived from this study and percent dry weight of crude terpenoids ($r^2=0.87$, n=8, $p < 0.001$) and crude fats ($r^2=0.86$, n=8, $p < 0.001$) derived from Kelsey et al. (1982)(Figure 3). As terpenoid and fat concentrations increase during the season, EF_{CO₂} increases. This is also supported by the large differences in the heat of combustion values between fats and terpenoids and sagebrush woody tissue in the literature. Typically, fats and terpenes/terpenoids have heat of combustion values; >2x those of sagebrush woody tissue (Hawkins and Eriksen, 1953; Van Epps et al., 1982). Higher heat of combustion values generally promote flaming combustion and greater EF_{CO₂} (Lobert and Warnatz, 1993). Despite these relationships, there are numerous factors influencing

emissions (e.g. fuel arrangement, climatic conditions, etc.), and we cannot conclusively state that foliar constituents are the primary driver in the EF_{CO_2} seasonality we observed.

Carbon budget analysis indicates that as the season progresses, increasingly more carbon is accounted for as CO_2 and less as CO (Figure 2e). This suggests that early season burns potentially produce more particulates and volatile organic compounds (VOCs), as the production of these emissions is strongly correlated to MCE (Yokelson et al., 2013). If the ratio of VOCs to NO_x is indeed greater in the early fire season, the production of ozone and photochemical smog via photolysis could be enhanced during this time period. Once the ratio exceeds (5.5:1), ozone production is usually intensified as less NO_x is removed from the system via the OH- NO_2 reaction and more NO_x is available for photolysis (Seinfeld and Pandis, 1998). Increased production of photochemical smog and $PM_{2.5}$ could deter resource managers from using prescribed fire in sagebrush ecosystems in the early fire season. On the contrary, higher MCE in the later fire season could be a better time to conduct prescribed burns as less pollutants are produced.

Conclusions

This study suggests that the seasonality does influence CO (weakly) and CO_2 (strongly) emission factors but does not influence the emission factors of NO, NO_2 , NO_x . The timing of sagebrush fires is therefore important for determining the potential of impaired air quality conditions, given the dry and cloud free conditions typically found in the Great Basin, United States. Application of constant emission factor values should be avoided and more research is warranted to re-test the synthesis results of Korontzi et al. (2003), which also showed carbonaceous seasonality emission factor trends in savannas, in other grass-dominant ecosystems. In addition to MCE, strong relationships ($r^2 > 0.86$) were observed between foliar constituents in the literature and CO_2 emission factors observed in this study, providing potential alternative mechanisms to describe combustion efficiency. This preliminary study also warrants further exploration of alternative ignition methods for big sagebrush at field moisture content as MCE and emission factors are strongly influenced by moisture content.

Acknowledgements

This work was partially funded by the National Aeronautics and Space Administration (NASA) under awards NNX11AO24G and NNX11AF19G.

References

- Akagi, S. K., Yokelson, R. J., Wiedinmyer, C., Alvarado, M. J., Reid, J. S., Karl, T., Crounse, J. D., and Wennberg, P. O. (2011). Emission factors for open and domestic biomass burning for use in atmospheric models. *Atmospheric Chemistry and Physics*, *11*, 4039-4072.
- Beck, J. L., Connelly, J. W., and Reese, K. P. (2009). Recovery of Greater Sage-grouse habitat features in Wyoming big sagebrush following prescribed fire. *Restoration Ecology*, *17*(3), 393-403.
- Beck, J. L., Connelly, J. W., and Wambolt, C. L. (2012). Consequences of treating Wyoming big sagebrush to enhance wildlife habitats. *Rangeland Ecology and Management*, *65*(5), 444-455.
- Burling, I. R., Yokelson, R. J., Griffith, D. W., Johnson, T. J., Veres, P., Roberts, J., Warneke, C., Urbanski, S. P., Reardon, J., Weise, D. R., Hao, W. M., and De Gouw, J. A. (2010). Laboratory measurements of trace gas emissions from biomass burning of fuel types from the southeastern and southwestern United States. *Atmospheric Chemistry and Physics*, *10*(22), 11115-11130.
- Clark, P. E., Lee, J., Ko, K., Nielson, R. M., Johnson, D. E., Ganskopp, D. C., Chigbrow, J., Pierson, F. B., and Hardegree, S. P. (2014) "Prescribed fire effects on resource selection by cattle in mesic sagebrush steppe. Part 1: Spring grazing." *Journal of Arid Environments*, *100*: 78-88.
- Crawford J.A., Olson R.A., West N.E., Mosley J.C., Schroeder M.A., Whitson T.D., Miller R.F., Gregg M.A., Boyd C.S. (2004). Synthesis paper – Ecology and management of sage-grouse and sage-grouse habitat, *Journal of Range Management*, *57*, 1, 2-19.
- Davies, K. W., Bates, J. D., & Miller, R. F. (2007). Short-term effects of burning Wyoming big sagebrush steppe in southeast Oregon. *Rangeland Ecology & Management*, *60*(5), 515-522.
- Davies, K. W., Bates, J. D., & Nafus, A. M. (2012). Comparing burned and mowed treatments in mountain big sagebrush steppe. *Environmental management*, *50*(3), 451-461.
- DePuit, E.J., and Caldwell, M.M. (1973). Seasonal pattern of net photosynthesis of *Artemisia tridentata*. *American Journal of Botany*, *60*(5), 426-435.
- DiTomaso, J. M., Brooks, M. L., Allen, E. B., Minnich, R., Rice, P. M., and Kyser, G. B. (2006). Control of Invasive Weeds with Prescribed Burning. *Weed Technology*. *20*:535-548.

- Evans, R. D., Black, R. A., Loescher, W. H., and Fellows, R. J. (1992). Osmotic relations of the drought-tolerant shrub *Artemisia tridentata* in response to water stress. *Plant, Cell & Environment*, 15(1), 49-59.
- Fernandez, O.A., and Caldwell, M.M. (1975). Phenology and dynamics of root growth of three cool semi-desert shrubs under field conditions. *Journal of Ecology*, 63(2), 703-714.
- Fischer, R. A., Reese, K. P., and Connelly, J. W. (1996). Influence of vegetal moisture content and nest fate on timing of female sage grouse migration. *Condor*, 98(4), 868-872.
- Fischer, R. A., Reese, K. P., and Connelly, J. W. (1996). An investigation on fire effects within xeric sage grouse brood habitat. *Journal of Range Management*, 194-198.
- Hardy, C., Ottmar, R., Peterson, J., Core, J., Seamon, P. (ed. 2001). *Smoke Management Guide for Prescribed and Wildland Fire*, National Wildfire Coordination Group. <http://www.nwcg.gov/pms/pubs/SMG/SMG-72.pdf>.
- Hawkins, J. E., and Eriksen, W. T. (1954). Physical and thermodynamic properties of terpenes. II. The heats of combustion of some terpene hydrocarbons. *Journal of the American Chemical Society*, 76(10), 2669-2671.
- Jaffe, D., Bertschi, I., Jaeglé, L., Novelli, P., Reid, J. S., Tanimoto, H., Vingarzan, R., and Westphal, D. L. (2004). Long-range transport of Siberian biomass burning emissions and impact on surface ozone in western North America, *Geophysical Research Letters*, 31(16).
- Kelsey, R.G., Stephens, J.R., and Shafizadeh, F. (1982). The chemical constituents of sagebrush foliage and their isolation. *Journal of Range Management*, 35(5), 617-622.
- Korontzi, S., Ward, D. E., Susott, R. A., Yokelson, R. J., Justice, C. O., Hobbs, P. V., Smithwick, E. A. H., and Hao, W. M. (2003). Seasonal variation and ecosystem dependence of emission factors for selected trace gases and PM_{2.5} for southern African savanna fires. *Journal of Geophysical Research: Atmospheres (1984–2012)*, 108(D24).
- Kuhlbusch, T. A., Lobert, J. M., Crutzen, P. J., and Warneck, P. (1991). Molecular nitrogen emissions from denitrification during biomass burning. *Nature*, 135-137.
- Lobert, J. M., and Warnatz, J. (1993). Emissions from the combustion process in vegetation. *Fire in the Environment: The Ecological, Climatic, and Atmospheric Chemical Importance of Vegetation Fires*, 15-37.
- Miller R.F., Knick S.T., Pyke D.A., Meinke C.W., Hanser S.E., Wisdom M.J., Hild A.L. (2011). Characteristics of sagebrush habitats and limitations to long-term

conservation. *Greater sage-grouse: ecology and conservation of a landscape species and its habitats. Studies in Avian Biology*, 38, 145-184.

Nelle, P. J., Reese, K. P., & Connelly, J. W. (2000). Long-term effects of fire on sage grouse habitat. *Journal of Range Management*, 586-591.

Pyle, W. H., & Crawford, J. A. (1996). Availability of foods of sage grouse chicks following prescribed fire in sagebrush-bitterbrush. *Journal of Range Management*, 320-324.

Rhodes, E. C., Bates, J. D., Sharp, R. N., & Davies, K. W. (2010). Fire Effects on Cover and Dietary Resources of Sage-Grouse Habitat. *The Journal of Wildlife Management*, 74(4), 755-764.

Seinfeld, J.H., and Pandis, S.N. (1998). *Atmospheric Chemistry and Physics: From Air Pollution to Climate Change*. John Wiley and Sons.

Sinha, P., Hobbs, P. V., Yokelson, R. J., Bertschi, I. T., Blake, D. R., Simpson, I. J., Gao, S., Kirchstetter, T. W., and Novakov, T. (2003). Emissions of trace gases and particles from savanna fires in southern Africa. *Journal of Geophysical Research*, 108, D13, 8487, doi:10.1029/2002JD002325.

Van Epps, G. A., Barker, J. R., and McKell, C. M. (1982). Energy biomass from large rangeland shrubs of the Intermountain United States. *Journal of Range Management*, 22-25.

Wilt, F.M., and Miller, G.C. (1992). Seasonal variation of coumarin and flavonoid concentrations in persistent leaves of Wyoming big sagebrush (*Artemisia tridentata* ssp. *Wyomingensis*: Asteraceae). *Biochemical Systematics and Ecology*, 20(1), 53-67.

Yokelson, R. J., Bertschi, I. T., Christian, T. J., Hobbs, P. V., Ward, D. E., and Hao, W. M. (2003). Trace gas measurements in nascent, aged, and cloud-processed smoke from African savanna fires by airborne Fourier transform infrared spectroscopy (AFTIR). *Journal of Geophysical Research*, 108, doi:10.1029/2002JD002322.

Table 1. Summary of big sagebrush moisture content, elemental analysis, and fuel consumption measurements (n = 110).

Date	Field Fuel Moisture (%)	C-content (%)	N-Content (%)	Fuel Consumption (%)
22-May	145.3 (6.5)	46.6 (0.64)	1.55 (0.09)	83.8 (3.51)
5-Jun	97.7 (8.0)	45.7 (1.94)	1.76 (0.23)	87.7 (3.03)
18-Jun	-	46.9 (0.59)	1.60 (0.17)	88.7 (3.08)
2-Jul	100.5 (8.7)	47.5 (0.69)	1.81 (0.12)	87.5 (5.91)
16-Jul	85.2 (4.7)	47.8 (0.28)	1.71 (0.11)	86.6 (4.41)
30-Jul	59.4 (3.5)	47.7 (0.99)	1.83 (0.10)	85.8 (3.63)
13-Aug	58.3 (6.3)	47.8 (0.55)	1.60 (0.04)	86.1 (3.17)
3-Sep	40.1 (4.8)	49.6 (0.16)	1.66 (0.27)	86.3 (2.92)
17-Sep	51.0 (4.1)	47.8 (2.01)	1.88 (0.14)	88.0 (0.91)
1-Oct	49.5 (4.8)	47.2 (1.23)	1.74 (0.20)	87.1 (4.12)
22-Oct	42.7 (5.4)	49.0 (0.58)	1.91 (0.08)	85.6 (2.04)

*Value in parentheses corresponds to (1σ) standard deviation.

Table 2. Relationships between CO₂ and CO emission factors (this study) and big sagebrush foliar constituents (Kelsey et al., 1982).

	EF CO₂	EF CO
Crude terpenoids	$y = 41.005x + 772.51$ $r^2 = 0.87, P < 0.001$	$y = -0.9445x + 97.48$ $r^2 = 0.44, P < 0.05$
Crude fat	$y = 49.255x + 1102.7$ $r^2 = 0.86, P < 0.001$	$y = -0.9324x + 88.83$ $r^2 = 0.32, P = 0.06$
Crude Protein	$y = -49.018x + 1897$ $r^2 = 0.44, P = 0.07$	$y = 1.0383x + 72.72$ $r^2 = 0.20, P = 0.167$
Total non-structural carbohydrates	$y = -50.458x + 2007.4$ $r^2 = 0.62, P < 0.05$	$y = 0.8662x + 72.79$ $r^2 = 0.23, P = 0.139$

*Foliar constituents in % dry weight.

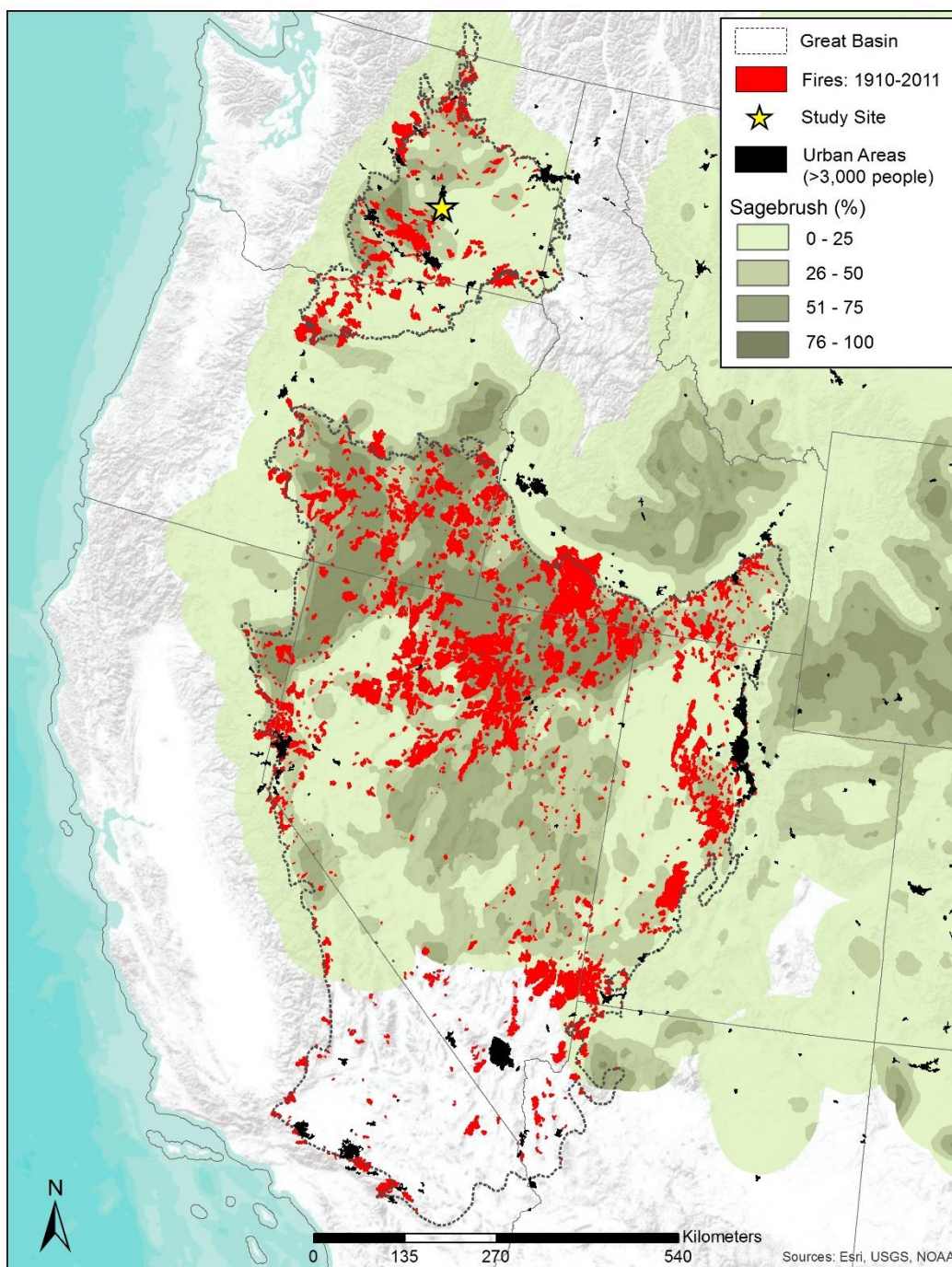


Figure 1. Extent of sagebrush in the Great Basin with fires from 1910-2011 with urban areas (>3,000 people) overlaid.

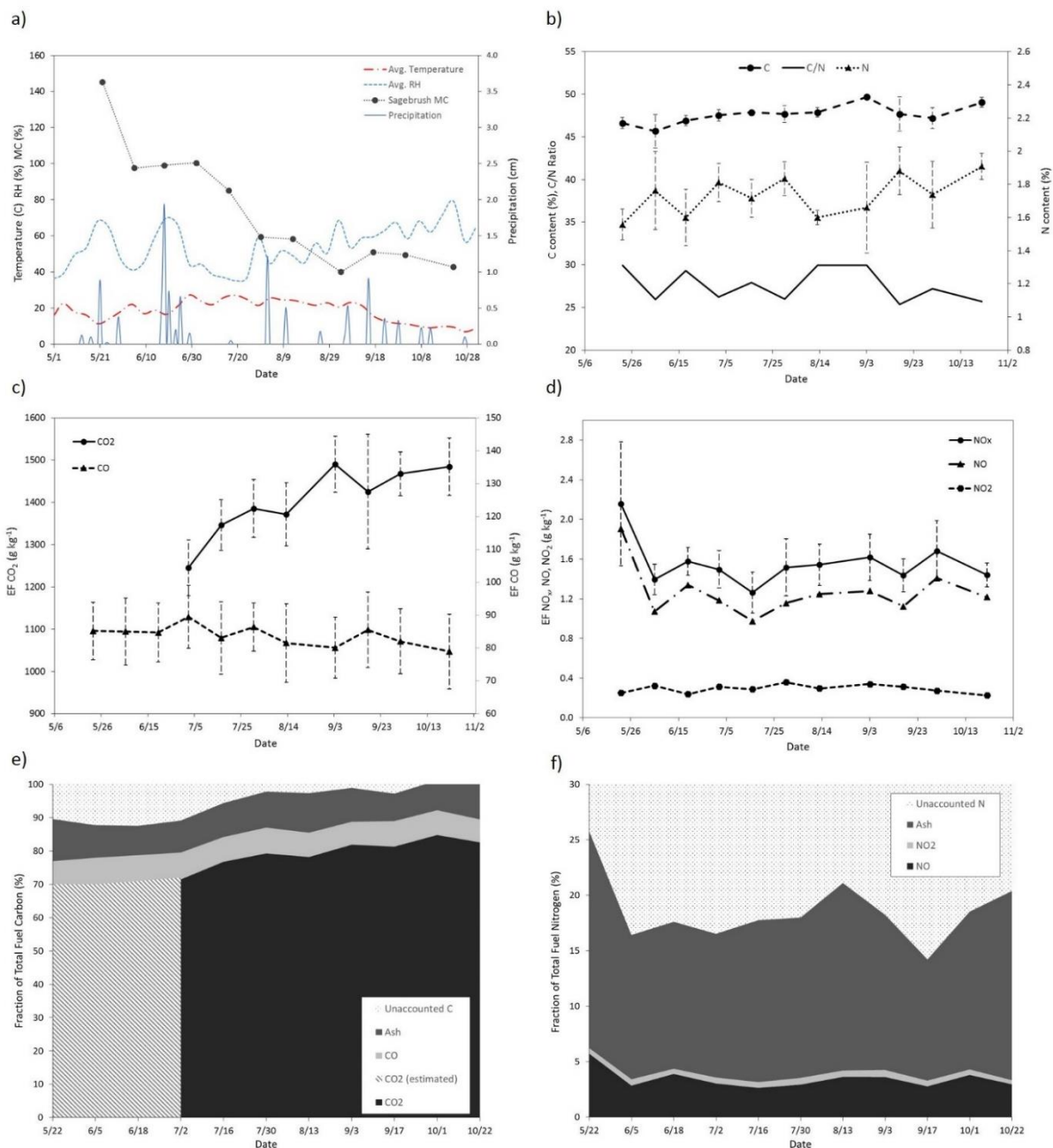


Figure 2. Emissions data including, a) climate data of study site (from Columbia National Wildlife Refuge RAWs station) and moisture content of sagebrush samples collected from May 5, 2013 to October 22, b) carbon and nitrogen content of samples, along with C:N ratio, c) seasonal CO₂ and CO emission factors, d) seasonal NO, NO₂, and NO_x emission factors, e) carbon balance, f) nitrogen balance.

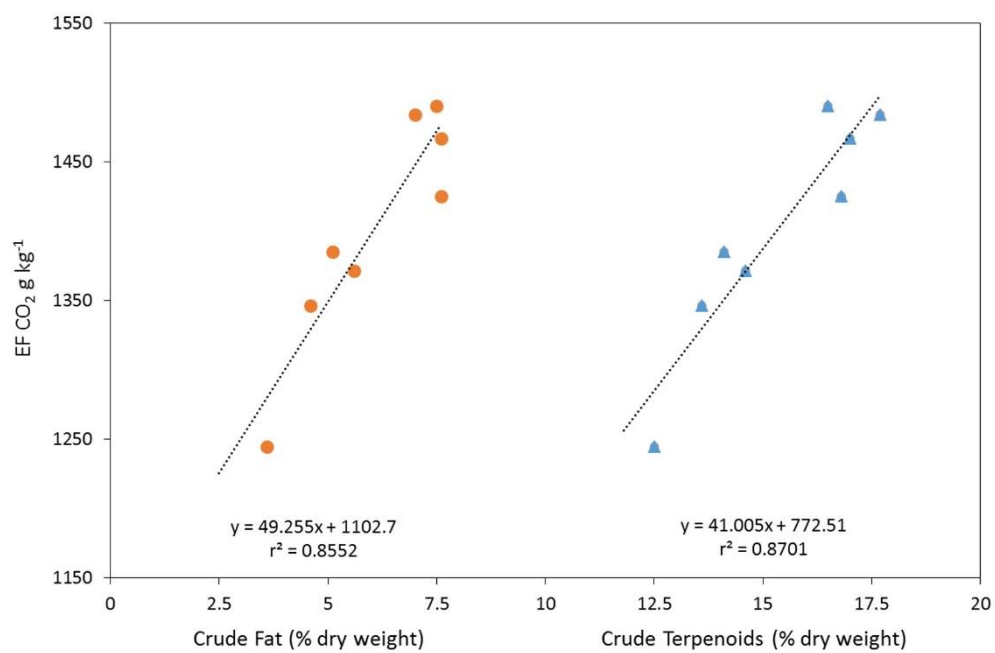


Figure 3. Relationships between EF_{CO₂} (this study) and sagebrush foliar crude fat and crude terpenoids (Kelsey et al., 1982).

Appendix A

Emissions Data from Shrub-steppe Fires: Bluebunch Wheatgrass and Cheatgrass

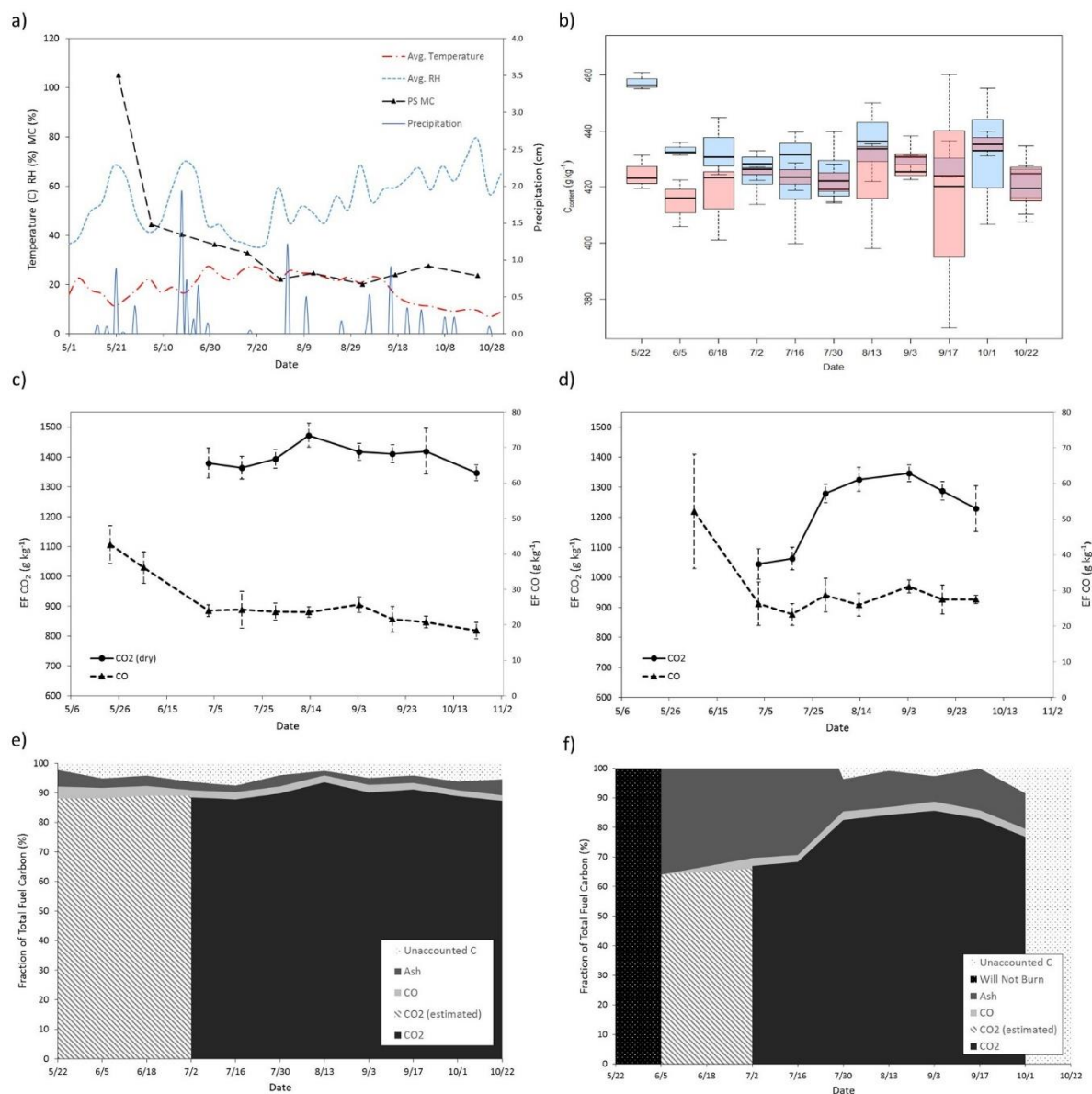


Figure 1. Emissions data including, a) climate data of study site (from Columbia National Wildlife Refuge RAWs station) and moisture content of bluebunch wheatgrass samples collected from May 5, 2013 to October 22, b) carbon content of samples (red = lower plant, blue = upper plant), along with C:N ratio, c) seasonal CO₂ and CO emission factors (samples burned dry), d) seasonal CO₂ and CO emission factors (samples burned at field moisture content (FMC)), e) carbon balance (samples burned dry), f) carbon balance (samples burned at FMC).

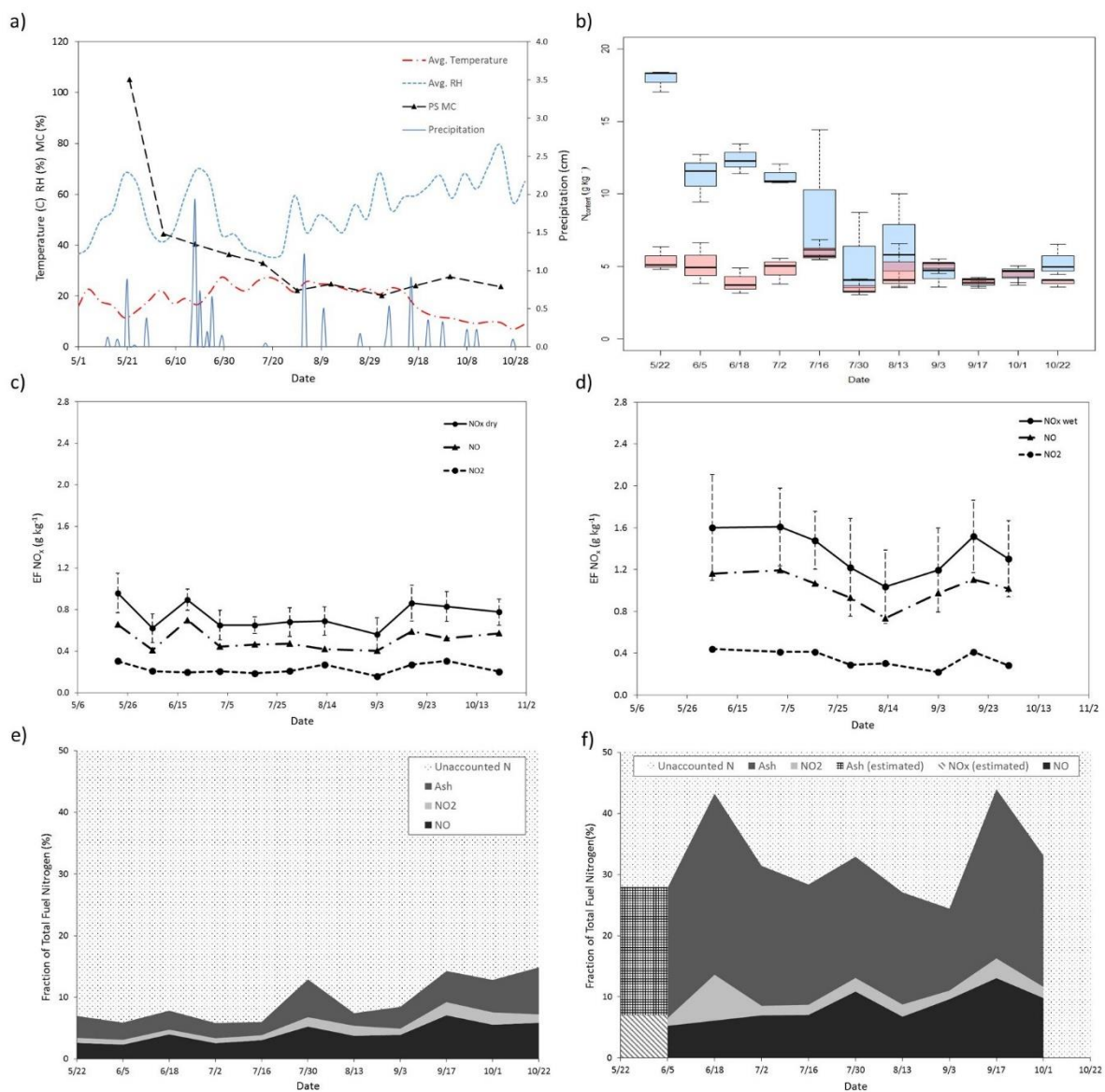


Figure 2. Emissions data including, a) climate data of study site (from Columbia National Wildlife Refuge RAWs station) and moisture content of bluebunch wheatgrass samples collected from May 5, 2013 to October 22, b) nitrogen content of samples (red = lower plant, blue = upper plant), along with C:N ratio, c) seasonal NO_x emission factors (samples burned dry), d) seasonal NO_x emission factors (samples burned at field moisture content (FMC)), e) nitrogen balance (samples burned dry), f) nitrogen balance (samples burned at FMC).

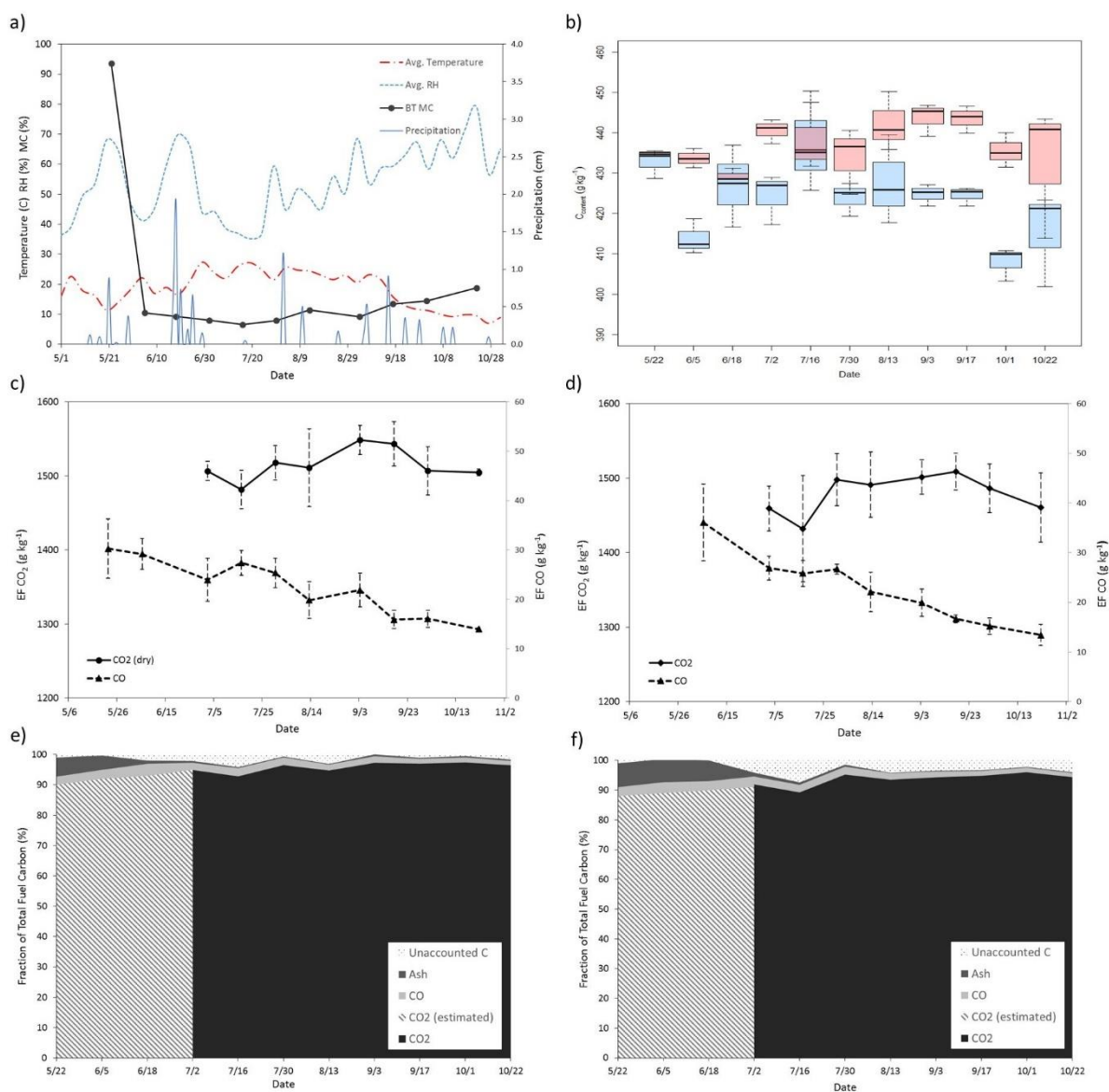


Figure 3. Emissions data including, a) climate data of study site (from Columbia National Wildlife Refuge RAWs station) and moisture content of cheatgrass samples collected from May 5, 2013 to October 22, b) carbon content of samples (red = lower plant, blue = upper plant), along with C:N ratio, c) seasonal CO₂ and CO emission factors (samples burned dry), d) seasonal CO₂ and CO emission factors (samples burned at field moisture content (FMC)), e) carbon balance (samples burned dry), f) carbon balance (samples burned at FMC).

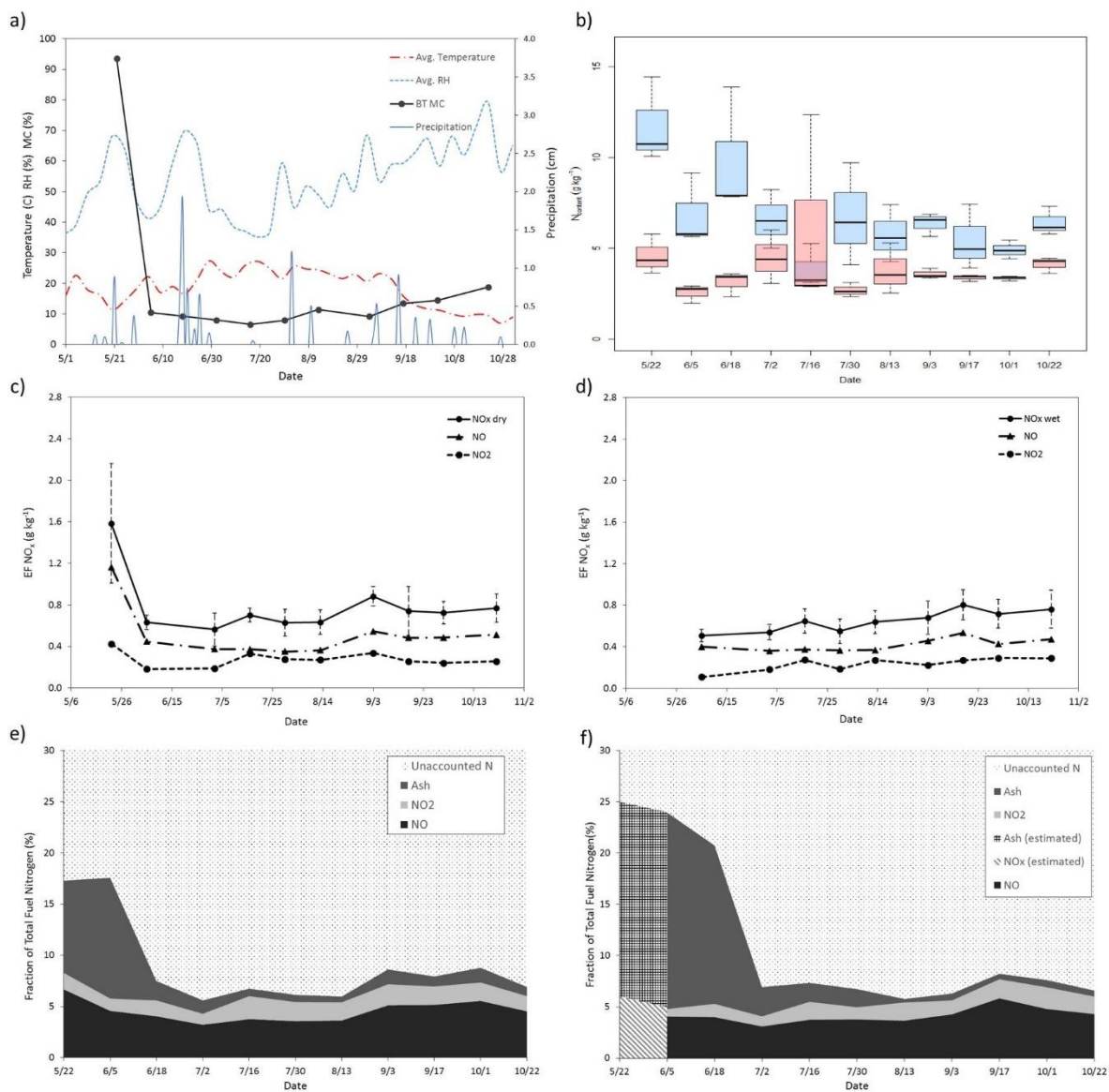


Figure 4. Emissions data including, a) climate data of study site (from Columbia National Wildlife Refuge RAWS station) and moisture content of cheatgrass samples collected from May 5, 2013 to October 22, b) nitrogen content of samples (red = lower plant, blue = upper plant), along with C:N ratio, c) seasonal NO_x emission factors (samples burned dry), d) seasonal NO_x emission factors (samples burned at field moisture content (FMC)), e) nitrogen balance (samples burned dry), f) nitrogen balance (samples burned at FMC).

Appendix B

Quantification of Fuel Moisture Effects on Biomass Consumed Derived from Fire Radiative Energy Retrievals

Quantification of Fuel Moisture Effects on Biomass Consumed Derived from Fire Radiative Energy Retrievals

Abstract

Satellite based fire radiant energy retrievals are widely applied to assess biomass consumed and emissions at regional to global scales. A known potential source of uncertainty in biomass burning estimates arises from fuel moisture but this impact has not been quantified in previous studies. Controlled fire laboratory experiments are used in this study to examine the biomass consumed and the radiant energy release (Fire Radiative Energy, FRE [MJ]) for western white pine needle fuels burned with water content (W_c , unitless) from 0.01 to 0.14. Results indicate a significant relationship: FRE per Kg of fuel consumed = $-5.32 W_c + 3.025$ ($r^2=0.83$, $n=24$, $p<0.001$) and imply that not taking into account fuel moisture variations in the assumed relationship between FRE and fuel consumed can lead to systematic biases. A methodological framework to derive a revised formula that enables the estimation of biomass consumed from FRE, which explicitly takes into account fuel water content, is presented.

Introduction

Biomass burning is a significant source of atmospheric trace gas and aerosol emissions, accounting globally for ~40% of annual carbon dioxide and carbon monoxide emissions [van der Werf *et al.*, 2010], although the exact quantities vary with inter-annual variability of climate processes [Slegert *et al.*, 2001; Littell *et al.*, 2009]. Quantifying biomass consumed and subsequent emissions is fundamental in understanding terrestrial-atmospheric Earth system processes and climate change [Bowman *et al.*, 2009]. Regional to global scale emission estimates are obtained conventionally via remotely sensed estimates of the area burned, model estimates of the quantity of fuel consumed, and the emission factors of the associated emitted greenhouse and trace gases [Crutzen and Andreae, 1990]. Recently, fire radiant energy remote sensing products from polar-orbiting and geostationary coarse resolution fire products have been applied to infer fire behavior and biomass consumed at regional to global scales [Kaufman *et al.*, 1998; Wooster, 2002; Roberts *et al.*, 2005; Smith and Wooster, 2005; Wooster *et al.*, 2005; Roberts and Wooster, 2008; Kumar *et al.*, 2011;

Kaiser et al., 2012; *Zhang et al.*, 2012; *Heward et al.*, 2013]. The fire radiant power (FRP) [units: W] retrieved at the time of satellite overpass is related to the instantaneous rate of biomass consumed; temporal integration of sampled FRP over the fire duration provides the Fire Radiative Energy (FRE) [units: J] which has been shown, with both laboratory and field measurements, to be linearly related to the amount of biomass burned [*Wooster*, 2002; *Wooster et al.*, 2005; *Freeborn et al.*, 2008; *Kremens et al.*, 2012].

A known potential source of uncertainty arises from water contained within the fuel but this impact has yet to be quantified by remote sensing FRE studies [*Brown and Davis*, 1973; *Freeborn et al.*, 2008; *Kremens et al.*, 2012; *Roy et al.*, 2013; *Wooster et al.*, 2013]. The fuel may not be completely dry when it is burned, depending on the precipitation and temperature regimes, the amount of drying due to the antecedent and current incoming solar radiation, the relative humidity of the atmosphere, condensation of dew onto the fuel surface, the state of decay of the fuels, and the proportion of live vegetation in the fuel. In terms of FRP measurement, the latent energy required to change the phase of liquid water in the fuel to water vapor (i.e., the enthalpy of vaporization) is not measured when sensing the combusting fuel within an actively burning fire. Moreover, the energy required to raise the liquid water in the fuel from ambient to boiling temperature and the energy required to drive the moisture out of the fuel (i.e., the heat of desorption) will reduce the emitted energy that is remotely sensed [*Brown and Davis*, 1973]. The emitted radiant energy may also be absorbed by water vapor and smoke in the atmospheric column between the fuel and the sensor and may be re-emitted in a direction away from the sensor. The combined impact of these loss mechanisms on fire radiant energy retrievals has yet to be quantified, which limits the confidence in using satellite derived radiant energy products for the assessment of regional to continental biomass consumed and emission estimates. Arguably these uncertainties, in addition to FRP sampling issues [*Boschetti and Roy*, 2008; *Kumar et al.* 2011], may have prevented a wider uptake of FRP based emission estimations. However, recent continental and global emission estimation systems that use FRP also rely on other data, for example, using empirical coefficients based on aerosol optical thickness retrievals [*Sofiev et al.* 2009] or, as in *Kaiser et al.*, [2012] normalizing the FRP-based emission retrievals against the Global Fire Emissions Database (GFED) which is produced using a conventional bottom-up emission estimation approach [*van der Werf et al.*, 2010]. For the

first time, we present results from a laboratory experiment to quantify how increasing moisture content impacts remotely sensed fire radiant energy retrievals.

Methodology

Experimental setup

Fire experiments were conducted at the Idaho Fire Institute of Research and Education (IFIRE) located in an indoor climatically controlled environment that is shielded from weather effects. Multiple approaches exist to estimate FRP, including single band mid-wave-infrared thermal imagers, dual-band thermometry, and Planck function curve fitting of 0.3 - 2.5 μm spectroradiometer data; the relative merits and the variation of FRP retrieved from these different methods are discussed in past studies [Dozier, 1981; Wooster *et al.*, 2005; Kremens *et al.*, 2010]. In this study, we used a dual-band infrared radiometer (0.15 – 11 μm and 6.5 - 20 μm) developed by the Rochester Institute of Technology to estimate FRP per unit area [W m^{-2}] at 0.5 second intervals using dual-band thermometry, where in contrast to single wavelength devices, measurements are acquired independently of emissivity [Kremens *et al.*, 2010, 2012]. As detailed in the literature [Dozier, 1981; Daniels, 2007; Kremens *et al.*, 2010, 2012], dual-band thermometry uses the principal that for a black- or grey-body radiation source the ratio of two infrared bands enables the kinetic temperature of the source to be estimated via a two point fit to the Planck function. The radiometer employs a ST60 dual-detector infrared thermopile [Dexter Research Center, MI] as an active element with custom noise filtering and amplifying electronics mounted on a printed circuit board in a ventilated fire resistant housing [Kremens *et al.*, 2012]. The system was radiometrically calibrated using standard blackbody radiation sources (Omega Engineering part # BB-4A and #BB-704) between 373K and 1250K [Wolfe and Zissis, 1993]. During operation, dry air was streamed across the dual-band infrared radiometer to reduce fouling due to soot and other smoke particulates. The ambient temperature of the dual-detector infrared thermopile was measured using a digital thermometer. The dual-band infrared radiometer has a 52° instrument field of view and was positioned at a fixed height of 1.16 m directly above the center of a 1 m^2 circular fuel bed so that the extent of the fuel bed was equal to the sensor field of view. To minimize the effects of conductive heat transfer the fuel bed was placed on a low conductivity fiber-glass mesh reinforced ceramic board. The board was placed on a

Sartorius EB Series scale (65 kg capacity, accurate to 1 g), synchronized with the dual-band radiometer to record fuel mass loss throughout the burn period. Fuels were collected from a single species western white pine (*Pinus monticola*) stand located adjacent to the University of Idaho, USA, and were manually sorted to remove impurities such as bark flakes, lichens, etc.

For each ignition, a small amount of lighter fluid was added to the edge of the fuel bed and ignited to provide a uniformly spreading flaming front. Each burn trial was considered complete once no mass loss was observed for at least 20 seconds. The radiometer recorded zero FRP values after the fire had extinguished, indicating the radiant energy emitted from the heated board was below the radiometer's detection limit. Prior to each ignition, all fuel beds were compressed to a constant bulk density of 85.7 kg m^{-3} to minimize variation in fire behavior and combustion completeness across the burn trials.

The FRE was derived as the discrete integral of the FRP over the duration of each burn:

$$FRE = \sum_{t_1}^{t_2} FRP_t \Delta t \quad [1]$$

where, t_1 [s] and t_2 [s] denote respectively the start and end of combustion, as defined above, FRP_t [W] is the power measured by the radiometer at time t and $\Delta t = 0.5 \text{ s}$ is the measurement sampling interval.

Fuel water content

Fuel moisture was quantified in terms of water content, defined as the percentage of water over the total mass of the (wet) sample:

$$W_c = \frac{W_M}{S_M} = \frac{W_M}{D_M + W_M} \quad [2]$$

where, W_c [dimensionless] is the fuel water content, S_M [Kg] is the total mass of the wet fuel sample, W_M [Kg] is the water mass, and D_M [Kg] is the dry mass of the fuel sample. The water content W_c is univocally related to the fuel moisture content (FMC), commonly used in the fire ecology community, which is defined as the water content (W_c) divided by the dry mass (D_M). The fuel moisture was controlled by reducing all material to $W_c < 0.01$ in an

oven, weighing the fuel beds to derive the dry mass, and then allowing the fuel to equilibrate outside the oven to the mass associated with the desired water content.

Theoretical Heat Budget

The radiant energy release fraction (f_r), defined as the fraction of total energy released during combustion in the form of radiation [Freeborn *et al.*, 2008], was calculated as:

$$f_r = \frac{FRE}{H_C * BC} \quad [3]$$

where H_C [MJ Kg⁻¹] is the heat of combustion, FRE [MJ] is defined via [1], and BC [Kg] is the total biomass consumed as measured by the scale.

A theoretical radiant heat budget per unit mass consumed was derived to independently quantify the deficit of retrieved fire radiant energy due to fuel moisture. The theoretical FRE released by a burnt sample is defined [Brown and Davis, 1973; Kremens *et al.*, 2012] as:

$$FRE = f_r * [H_C D_M - W_M (H_{vap} + c_w (373 - T_a) + H_{Des})] \quad [4]$$

where, f_r is defined as [3], H_C is the heat of combustion of pine needles (20.138 MJ Kg⁻¹, Font *et al.*, 2009), D_M is the dry mass of the sample, W_M is the water content of the sample, H_{vap} is the enthalpy of water vaporization at atmospheric pressure (2.257 MJ Kg⁻¹), C_w is the heat capacity of water (0.0042 MJ Kg⁻¹), T_a = ambient temperature (300K), and H_{Des} is the heat of desorption = 0.1 MJ Kg⁻¹ [Brown and Davis, 1973; Shottafer and Shuler, 1974].

Rearranging the terms of [4], substituting [2], and normalizing for mass, provides:

$$\frac{FRE}{BC} = f_r [H_C - W_C (H_C + H_{vap} + c_w (373 - T_a) + H_{Des})] \quad [5]$$

which can be simplified into a general equation that expresses the relationship between FRE, BC, and W_C as:

$$BC = (b - m * W_C)^{-1} * FRE \quad [6]$$

where, b [MJ Kg⁻¹] is the FRE emitted per unit of biomass consumed by a dry fuel (0 W_C), and m is any bias in the FRE per unit of biomass due to change in W_C .

Experimental burns

An initial set of 15 dry ($< 0.01 W_c$) needle fuel beds were created, with a range of fuel loads from 100 to 500 g m⁻² to test the conventional biomass consumed FRE relationship described by *Wooster et al.* [2005] as:

$$BC_{Wooster} = 0.368(\pm 0.015) * FRE \quad [7]$$

where, $BC_{wooster}$ is the biomass consumed [Kg] and FRE [MJ] is derived from [1]. *Wooster et al.* [2005] derived this relationship from the combustion of *Miscanthus* grasses with ~0.12 moisture content sensed with a MWIR imager. Using the experimental FRE and BC data from the combustion of the 15 dry fuel beds, the slope coefficient of [7], together with its 95% confidence interval, was estimated by linear regression. The radiant energy release fraction (f_r) was also determined for each of the 15 dry fuel burns using [3] and an average calculated.

Subsequently, 24 pine needle fuel beds were burned with W_c ranging from 0.01 to 0.14. A dry fuel load of 300 g m⁻² was used for each of these 24 burns to reflect typical conifer *Pinus* spp. forest needle fuel loading [*Nelson and Heirs, 2008*]. The measured W_c , BC, and retrieved FRE were used to estimate the terms m and b in [6] by linear regression.

Results and Discussion

Fig. 1 compares the biomass consumed of dry pine needles with the retrieved fire radiant energy (closed circles) and demonstrates a strong ($r^2=0.998$, $n=15$, $p<0.001$) linear relationship, with a 0.325 ± 0.008 slope. The observed variability in the plotted data is attributed to differences in the fuel bed bulk density and homogeneity of the fuel load among the 15 experimental dry burns. The pine needle radiant energy release fraction (f_r) was $14.7 \pm 1\%$ and is comparable to values observed by other researchers for *Miscanthus* grass ($f_r = 13 \pm 3\%$ [*Wooster et al., 2005*]), mixed fuel beds of needles and wood ($f_r = 11.7 \pm 2.4\%$ [*Freeborn et al., 2008*]), and oak savannah litter ($f_r = 17 \pm 3\%$ [*Kremens et al., 2012*]). The dashed line shows the biomass consumed predicted from the retrieved FRE using the conventional relationship described by [7]. Differences in the slope functions can be attributed to the fuel type, the moisture content of the fuel, and the experimental approach (i.e. dual-band thermometry vs. MWIR imager). Specifically, *Wooster et al.* [2005] used

Miscanthus grass that has a lower heat of combustion ($H_C = 17.100\text{-}19.400 \text{ MJ Kg}^{-1}$) compared to the pine needles ($20.138 \text{ MJ Kg}^{-1}$) and the grass had $W_c \sim 0.12$.

Fig. 2 compares the ratio of the FRE to the biomass consumed with the water content (closed circles). The retrieved FRE decreases with increasing moisture content. A significant relationship is observed: FRE per Kg of fuel consumed = $-5.32 W_c + 3.025$ ($r^2=0.83$, $n=24$, $SE = 0.104$, $p<0.001$). The regression coefficient standard errors were one and two orders of magnitude smaller than the regression coefficient values (standard errors of 0.5 and 0.038 for the gradient and intercept coefficients respectively). The observed variability in the plotted data around the regression line is most likely due to experimental measurement error (radiometer, mass scale and W_c). The theoretical radiant heat budget per unit mass consumed [4] is shown on Fig 2. (dashed line) and indicates general agreement, within the range of the variability of the observed data. The absolute mean difference between the theoretical and observed values across the range of W_c was 0.13 with a standard deviation of 0.09 MJ Kg^{-1} . This difference is likely due to errors in the parameterization of [4], for example, the heat of desorption is not particularly well defined in the literature, or due to an additional unaccounted for processes such as the absorption of emitted energy by water vapor and smoke in the atmospheric column [Brown and Davis, 1973; Freeborn et al., 2008].

The 24 measured W_c , BC, and retrieved FRE values were used to estimate the terms b and m in [6] by linear regression to provide $b = 3.025 \text{ [MJ Kg}^{-1}\text{]}$ and $m = 5.32$ with 95% confidence intervals ± 0.079 and ± 0.0105 respectively. This provides:

$$BC = (3.025 - 5.32 * W_c)^{-1} * FRE \quad [8]$$

where, BC [Kg] is the total biomass consumed and FRE [MJ] is the fire radiative energy. Equation [8] enables the estimation of biomass consumed from FRE explicitly taking into account fuel water content and updates the conventional biomass consumed FRE relationship described by Wooster et al. [2005] and [7].

Fig. 3 shows the results of the application of [8] for water content ranging from 0 to 0.25 applied to the 15 dry fuel FRE values illustrated in Fig 1. Clearly, changes in fuel moisture will bias conventional biomass burning estimates from FRE [7]. It should be noted that

while pine needles do not combust at $W_c \sim 0.26$, peat and other fuels can combust at significantly higher moisture contents [Benscoter *et al.*, 2011], potentially making the impact of fuel water content on FRE biomass burned retrieval even more pronounced for these fuel types. Comparison of [8] to [7], which was parameterized at $W_c \sim 0.12$, yields a 14% difference in the gradient. This difference can be partly attributed to the variations in the heat of combustion, time from W_c calculation to combustion, and the different FRP retrieval methods [Wooster *et al.*, 2003, 2005].

Conclusions

This research confirms past studies showing strong linear relationships between biomass consumed and integrated fire radiant energy. Measurements from two sets of experimental burns were used to quantify the impact of fuel water content on fire radiant energy, and to derive a new formula where the linear relationship between biomass consumed and fire radiant energy is parameterized for fuel water content. Comparison of these results to past studies demonstrates that dual-band thermometry produces data of comparable accuracy and precision to other FRP retrieval approaches. The results of this study have several implications for the future use of satellite based fire energy retrievals to estimate biomass consumed. Conventional biomass burning retrievals, using the equation proposed by Wooster *et al.* [2005], do not take into account fuel moisture, and may systematically bias estimates of the biomass consumed. This is particularly relevant given that the fuel moisture may change through the fire season and the seasonality of fire extent and intensity remains an area of active research [Korontzi *et al.*, 2004; Roy *et al.*, 2005; Yates *et al.*, 2008; Archibald *et al.*, 2010; Meyer *et al.*, 2012; Randerson *et al.*, 2012].

This study suggests the need to test whether similar moisture content relationships are observed for diverse fuels such as in peat, woody debris, and leaf litter [Hyde *et al.*, 2011; Kremens *et al.*, 2012; Brewer *et al.*, 2013]. Moisture-corrected FRE biomass burned equations would improve the application of spaceborne fire radiant energy products in assessing biomass burning but this application will require spatially and temporally explicit estimation of fuel moisture. Future research to further validate the methodology is recommended. This should include cross-comparison of single band and dual-band FRP approaches to further evaluate moisture effects on FRP [Wooster *et al.*, 2005] and the

application of the method to satellite FRP data and fuel stratification maps to determine fuel-type specific coefficients for [6]; thus enabling systematic moisture content corrections for FRE to be realized.

Acknowledgements

This work was partially supported by the NSF Idaho EPSCoR Program and by the National Science Foundation under award number EPS-0814387. Partial funding support was received via Joint Fire Sciences Program under award number 07-2-1-60 and the National Aeronautics and Space Administration (NASA) under awards NNX11AO24G, NNX12AK31G and NNX11AF39G.

References

- Archibald, S., R.J. Scholes, D.P. Roy, G. Roberts, and L. Boschetti (2010), Southern African fire regimes as revealed by remote sensing, *International Journal of Wildland Fire*, 19, 861–878.
- Benscoter, B.W., D.K. Thompson, J.M. Waddington, M.D. Flannigan, B.M. Wotton, W.J. de Groot, and M.R. Turetsky. (2011), Interactive effects of vegetation, soil moisture and bulk density on depth of burning of thick organic soils, *International Journal of Wildland Fire*, 20, 418-429.
- Boschetti L. and Roy, D.P., 2009, Strategies for the fusion of satellite fire radiative power with burned area data for fire radiative energy derivation, *Journal of Geophysical Research Atmospheres*, 114, D20302, doi:10.1029/2008JD011645.
- Bowman, D., J. Balch, P. Artaxo, W. Bond, J. Carlson, M. Cochrane, C. D’Antonio, R. DeFries, J. Doyle, S. Harrison, F. Johnston, J. Keeley, M. Krawchuk, J. Marston, M. Moritz, I. Prentice, C. Roos, A. Scott, T. Swetnam, G. van der Werf, and S. Pyne (2009), Fire in the Earth System, *Science*, doi:10.1126/science, 1163886.
- Brewer, N.W., A.M.S. Smith, P.E. Higuera, J.A. Hatten, A.T. Hudak, R.D. Ottmar, W.T. Tinkham, and R.L. Kremens (2013), Fuel moisture influence on fire-altered carbon in masticated fuels: an experimental study, *Journal of Geophysical Research*, 118, 30-40, doi: 10.1029/2012JG002079.
- Brown, A.A. and K.P. Davis (1973), *Forest Fire: Control and Use*, Second Edition, McGraw-Hill Book Company, New York, ISBN: 0-07-008205-7, pp155-182.
- Crutzen, P.J., and M.O. Andreae (1990), Biomass burning in the tropics: Impact on atmospheric chemistry and biogeochemical cycles, *Science*, 250 (4988), 1669-1678, doi: 10.1126/science.250.4988.1669.
- Daniels, A. (2007). *Field guide to infrared systems*. SPIE Publishing, Bellingham, Washington, USA.
- Dozier, J. (1981). A method for satellite identification of surface temperature fields of sub-pixel resolution. *Remote Sensing of Environment*, 11, 221– 229.
- Font, R., J.A. Conesa, and J.M.M. Munoz (2009), Kinetics of pyrolysis and combustion of pine needles and cones, *Journal of Analytical and Applied Physics*, 85, 276-286.
- Freeborn, P.H., M.J. Wooster, W. Min Hao, C.A. Ryan, B.L. Hordgren, S.P. Baker, and C. Ichoku (2008), Relationships between energy release, fuel mass loss, and trace gas and aerosol emissions during laboratory biomass fires, *Journal of Geophysical Research*, 113, D01301, doi: 10.1029/2007JD008679.
- Heward H., A.M.S. Smith, D.P. Roy, W.T. Tinkham, C.M. Hoffman, P. Morgan, and K.O. Lannom, (2013), Is burn severity related to fire intensity? Observations from landscape

- scale remote sensing, *International Journal of Wildland Fire*, 22, 7, 910-918, doi: 10.1071/WF12087.
- Hyde, J.C., A.M.S. Smith, R.D. Ottmar, E.C. Alvarado, and P. Morgan (2011), The Combustion of Sound and Rotten Coarse Woody Debris: A Review, *International Journal of Wildland Fire*, 20, 163-174
- Kaiser, J.W., A. Heil, M.O. Andreae, A. Benedetti, N. Chubarova, L. Jones, J.-J. Morcrette, M. Razinger, M.G. Schultz, M. Suttie, and G.R. van der Werf (2012), Biomass burning emissions estimated with a global fire assimilation system based on observed fire radiative power, *Biogeosciences*, 9, 527-554, doi: 10.5194/bg-9-527-2012.
- Kaufman, Y.J., P.V. Hobbs, V.W.J.H. Kirchhoff, P. Artaxo, L.A. Remer, B.N. Holben, M.D. King, D.E. Ward, E.M. Prins, K.M. Longo, L.F. Mattos, C.A. Nobre, J.D. Spinhirne, Q. Ji, A.M. Thompson, J.F. Gleason, S.A. Christopher, S.-C. Tsay (1998), Smote, Clouds, and Radiation-Brazil (SCAR-B) experiment, *Journal of Geophysical Research: Atmospheres*, 103, D24, 31783-31808, doi: 10.1029/98JD02281.
- Korontzi, S., D.P. Roy, C.O. Justice, and D.E. Ward (2004), Modeling and sensitivity analysis of fire emissions in southern Africa during SAFARI 2000, *Remote Sensing of Environment*, 92, 255-275.
- Kremens, R.L., A.M.S. Smith, and M.B. Dickinson (2010), Fire Metrology: Current and future directions in physics-based measurements, *Fire Ecology*, 6, 13-35
- Kremens, R.L., M.B. Dickinson, and A.S. Bova (2012), Radiant flux density, energy density and fuel consumption in mixed-oak forest surface fires, *International Journal of Wildland Fire*, doi: 10.1071/WF10143.
- Kumar, S.S., D.P. Roy, L. Boschetti, and R. Kremens (2011), Exploiting the power law distribution properties of satellite fire radiative power retrievals - a method to estimate fire radiative energy and biomass burned from sparse satellite observations, *Journal of Geophysical Research*, 116, D19303, doi: 10.1029/2011JD015676.
- Littell, J.S., D. McKenzie, D.L. Peterson, and A.L. Westerling (2009), Climatic influences on twentieth-century area burned in ecoprovinces of the western U.S., *Ecological Applications*, 19, 4, 1003-021, doi: 10.1890/07-1183.1.
- Meyer, M.C.P., G.D. Cook, F. Reisen, T.E.L. Smith, M. Tattaris, J. Russell-Smith, W.M. Stefan, C.P. Yates, and M.J. Wooster (2012), Direct measurements of the seasonality of emission factors from savanna fires in northern Australia, *Journal of Geophysical Research - Atmospheres*, 117, D20305, doi:10.1029/2012JD017671.
- Nelson, R.M and J.K. Heirs (2008), The influence of fuelbed properties on moisture drying rates and timelags of longleaf pine litter. *Canadian Journal of Forest Research*, 38, 2394-2404.

- Randerson, J.T., Y. Chen, G.R. van der Werf, B.M. Rogers, and D.C. Morton (2012), Global burned area and biomass burning emissions from small fires, *Journal of Geophysical Research*, *117*, G04012, doi: 10.1029/2012JG002128.
- Roberts G.J., M.J. Wooster, G.L.W. Perry, N. Drake, L.-M. Rebelo, and F. Dipotso (2005), Retrieval of biomass combustion rates and totals from fire radiative power observations: Application to southern Africa using geostationary SEVIRI imagery, *Journal of Geophysical Research*, *110*, D21111, doi: 10.1029/2005JD006018.
- Roberts, G.J. and M.J. Wooster (2008), Fire detection and fire characterization over Africa using Meteosat SEVIRI, *IEEE Transactions on Geoscience and Remote Sensing*, *46*(4), 1200-1218.
- Roy, D.P., P. Frost, C. Justice, T. Landmann, J. Le Roux, K. Gumbo, S. Makungwa, K. Dunham, R. Du Toit, K. Mhwandagara, A. Zacarias, B. Tacheba, O. Dube, J. Pereira, P. Mushove, J. Morissette, S. Vannan, and D. Davies (2005), The Southern Africa Fire Network (SAFNet) regional burned area product validation protocol, *International Journal of Remote Sensing*, *26*, 4265-4292.
- Roy, D.P., L. Boschetti, and A.M.S. Smith, Satellite remote sensing of fires, chapter 5 in Belcher, C.M. and Rein, G., eds., *Fire Phenomena and the Earth System: An Interdisciplinary Guide to Fire Science*, John Wiley & Sons, Ltd., Chichester, England, 368pp. ISBN: 978-0-470-65748-5. doi: 10.1002/9781118529539.ch5, 2013
- Shottafer, J.E. and C.E. Shuller (1974) Estimating heat consumption in kiln drying lumber, Life Sciences and Agriculture Experiment Station, Technical Bulletin 73, University of Maine, 25pp.
- Slegert, F., G. Ruecker, A. Hinrichs, and A.A. Hoffmann (2001), Increased damage from fires in logged forests during droughts caused by El Nino, *Nature*, *414*, 437-440, doi: 10.1038/35106547.
- Smith A.M.S. and M.J. Wooster (2005), Remote classification of head and backfire types from MODIS fire radiative power observations, *International Journal of Wildland Fire*, *14*, 249-254.
- Sofiev M., Vankevich, R., Lotjonen, M., Prank, M., Petukhov, V., Ermakova, T., Koskinen, J., Kukkonen, J. (2009) An operational system for the assimilation of the satellite information on wild-land fires for the needs of air quality modelling and forecasting, *Atmospheric Chemistry and Physics*, *9*, 6833-6847.
- van der Werf, G.R., J.T. Randerson, L. Giglio, G.J. Collatz, M. Mu, P.S. Kasibhatla, D.C. Morton, R.S. DeFries, Y. Jin, and T.T. van Leeuwen (2010), Global fire emissions and the contribution of deforestation, savanna, forest, agricultural, and peat fires (1997-2009), *Atmospheric Chemistry and Physics*, *10*, 11707-35.
- Wolfe, W.L. and G.J. Zissis (1993), *The Infrared Handbook*. General Dynamics, 1700pp ISBN: 096035901X.

- Wooster, M.J. (2002), Small-scale experimental testing of fire radiative energy for quantifying mass combusted in natural vegetation fires, *Geophysical Research Letters*, 29(21), 2027, doi: 10.1029/2002GL015487.
- Wooster M.J., Zhukov, B. and Oertel, D (2003), Fire radiative energy for quantitative study of biomass burning: derivation from the BIRD experimental satellite and comparison to MODIS fire products, *Remote Sensing of Environment*, 86, 83-107. doi: 10.1016/S0034-4247(03)00070-1.
- Wooster M.J. and Y.H. Zhang (2004), Boreal forest fires burn less intensely in Russia than in North America, *Geophysical Research Letters*, 31, L20505, doi: 10.1029/2004GL020805.
- Wooster, M.J., G. Roberts, G.L.W. Perry, and Y.J. Kaufman (2005), Retrieval of biomass combustion rates and totals from fire radiative power observations: FRP derivation and calibration relationships between biomass consumption and fire radiative energy release, *Journal of Geophysical Research-Atmospheres*, 110, D24311, doi: 10.1029/2005JD006318.
- Wooster, M.J., G. Roberts, A.M.S. Smith, J. Johnson, P. Freeborn, S. Amici, and A.T. Hudak, Thermal Remote Sensing of Active Vegetation Fires and Biomass Burning Events, chapter 18, in "*Thermal Remote Sensing*", Eds: C. Kuenzer and S. Dech. Springer, ISBN: 978-94-007-6638-9. 2013
- Yates, C.P., A.C. Edwards, and J. Russell-Smith (2008), Big fires and their ecological impacts in Australian savannas: size and frequency matters, *International Journal of Wildland Fire*, 17, 768–781.
- Zhang, X., S. Kondragunta, J. Ram, C.C. Schmidt, and H.-C. Huang (2012), Near real time global biomass burning emissions product from geostationary satellite constellation, *Journal of Geophysical Research*, 117, D14, doi: 10.1029/2012JD017459.

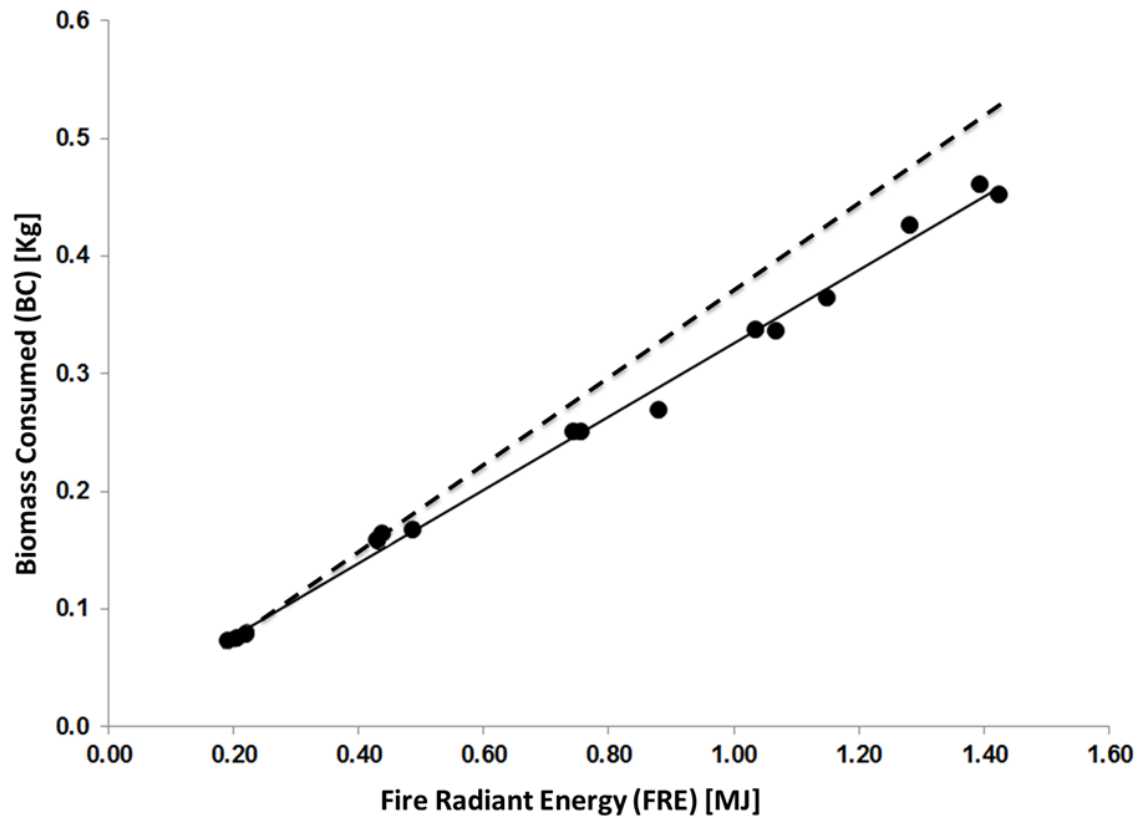


Figure 1. Relationship between fire radiant energy (FRE) biomass consumed (BC) for 15 dry ($<0.01 W_C$) pine needle experimental burns (closed circles). The best-fit linear regression passing through the origin ($BC=(0.325\pm 0.008)*FRE$, $r^2=0.998$, $n=15$, $p<0.01$) is shown as a continuous line. The dashed line shows the BC predicted from the retrieved FRE using the conventional relationship described by [7].

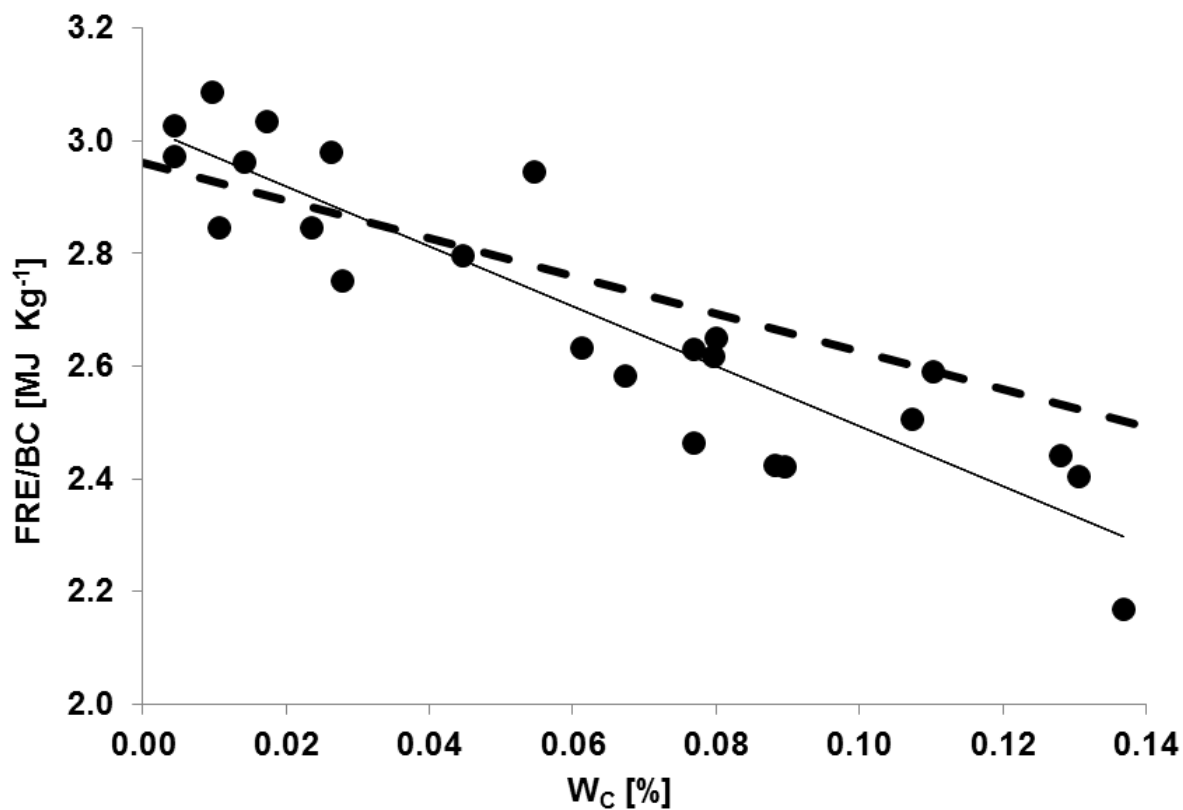


Figure 2. The impact of water content, W_C , on the FRE per unit of biomass consumed (FRE/BC) for 24 experimental burns (closed circles). The regression of these data (solid line) is: $\text{FRE/BC (MJ Kg}^{-1}\text{)} = -5.32W_C + 3.025$ ($r^2=0.832$, $n=24$, $p<0.001$). The 95% confidence intervals for the gradient and intercept are ± 0.0105 and ± 0.079 respectively. The theoretical radiant heat budget per unit mass consumed [4] is shown as a dashed line.

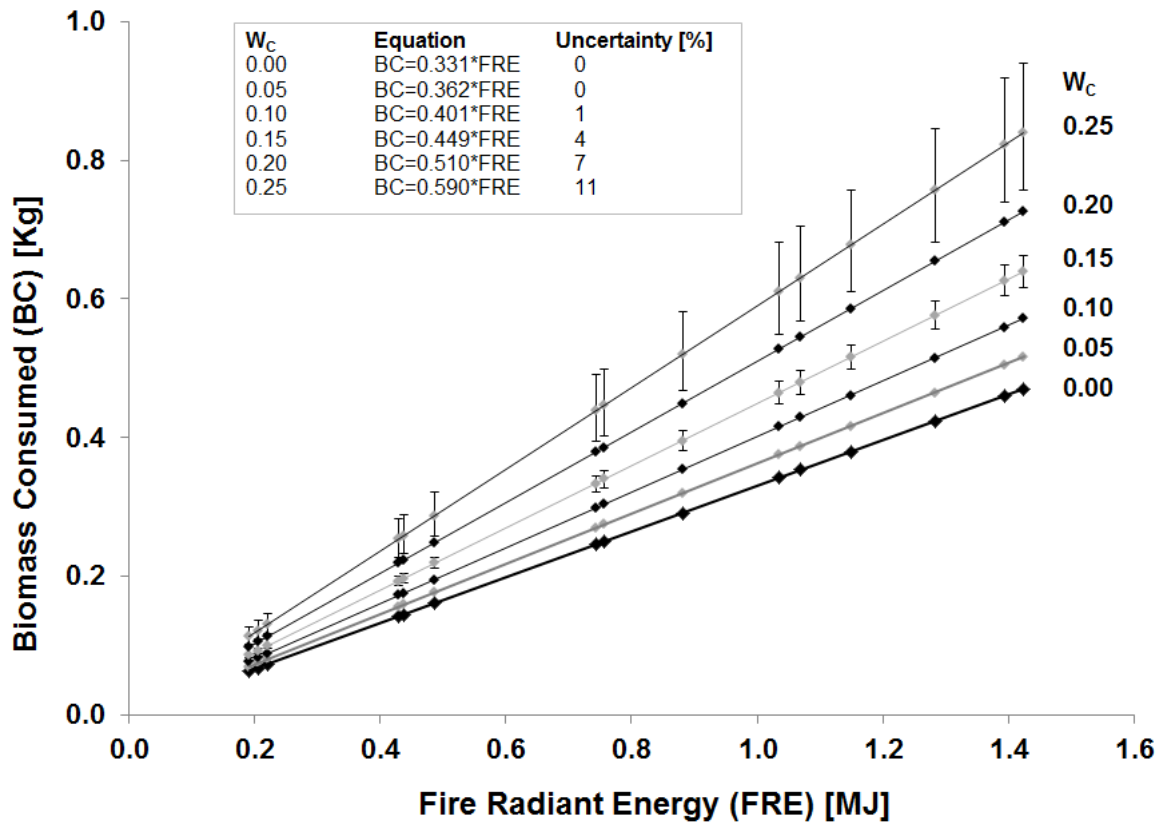


Figure 3. Impact of fuel water content W_c (dimensionless), on the relationship between retrieved FRE and biomass consumed (BC). Equation [8] is theoretically demonstrated for W_c values from 0-0.25 for the 15 dry pine fuel FRE retrievals illustrated in Fig. 1, and the resulting linear equations are plotted as diagonal lines. The % uncertainty is calculated for each W_c line by applying the 95% confidence intervals from the gradient and intercept coefficients in [8]. Only the error bars associated with 0.15 and 0.25 are shown for illustrative purposes. Pine needles do not burn if the water content is higher than ~ 0.26 . The reported equations values are derived from the current experimental data and are in close correspondence to the theoretical values that can be derived from [5].